Residential building stock modeling for mainland China targeted for seismic risk assessment

Danhua Xin[1,2,*], James Edward Daniell[2,3,*], Hing-Ho Tsang[4], Friedemann Wenzel[2]

[1]Department of Earth and Space Sciences, Southern University of Science and Technology, 1088 Xueyuan Avenue, Shenzhen 518055, Guangdong Province, China

[2]Center for Disaster Management and Risk Reduction Technology (CEDIM) and Geophysical Institute, Karlsruhe Institute of Technology, Hertzstrasse 16, 76187, Karlsruhe, Germany

[3]General Sir John Monash Scholar, The General Sir John Monash Foundation, Level 5, 30 Collins Street, Melbourne, Victoria, 3000, Australia

[4]Centre for Sustainable Infrastructure, Swinburne University of Technology, Melbourne, VIC 3122, Australia

[*]*Correspondence to* James Edward Daniell (j.e.daniell@gmail.com), Danhua Xin (xindh@sustech.edu.cn)

Abstract

To enhance the estimation accuracy of economic loss and casualty in seismic risk assessment, a high-resolution building exposure model is necessary. Previous studies in developing global and regional building exposure models usually use coarse administrative level (e.g., country, or sub-country level) census data as model inputs, which cannot fully reflect the spatial heterogeneity of buildings in large countries like China. To develop a high-resolution residential building stock model for mainland China, this paper uses finer urbanity level population and building-related statistics extracted from the records in Tabulation of the 2010 Population Census of the People's Republic of China (hereafter abbreviated as the "2010-census"). In the 2010-census records, for each province, the building-related statistics are categorized into three urbanity levels (urban, township, and rural). To disaggregate these statistics into high-resolution grid level, we need to determine the urbanity attributes of grids within each province. For this purpose, the geo-coded population density profile (with 1km×1km resolution) developed in the 2015 Global Human Settlement Layer (GSHL) project is selected. Then for each province, the grids are assigned with urban/township/rural attributes according to the population density in the 2015 GHSL profile. Next, the urbanity level building-related statistics can be disaggregated into grids, and the 2015 GHSL population in each grid is used as the disaggregation weight. Based on the four structure types (steel/reinforced-concrete, mixed, brick/wood, other) and five storey classes (1, 2-3, 4-6, 7-9, ≥10) of residential buildings classified in the 2010-census records, we reclassify the residential buildings into 17 building subtypes attached with both structure type and storey class and estimate their unit construction prices. Finally, we develop a geo-coded 1km×1km resolution residential building exposure model for 31 provinces of mainland China. In each 1km×1km grid, the floor areas of the 17 residential building subtypes and their replacement values are estimated. The model performance is evaluated to be satisfactory, and its practicability in seismic risk assessment is also confirmed. Limitations of the proposed model and directions for future improvement are discussed. The whole modeling process presented in this paper is fully reproducible, and all the modeled results are publicly accessible.

Key Words: residential building stock modeling, 2010-census records, dasymmetric disaggregation

1. Introduction

The frequent occurrence of earthquakes and other natural hazards (typhoon, flood, tsunami, etc.) can lead to tremendous and often crippling economic losses. According to the estimation in Daniell et al. (2017), from 1900-2016, 2.3 million earthquake fatalities from 2233 fatal events occurred worldwide. Economic losses (direct and indirect) associated with the occurrence of over 9,900 damaging earthquakes reached USD 3.41 trillion (in 2016 prices). For cases in China, the combination of high seismic activity, population density, and building vulnerability cause even higher seismic risk: Earthquakes that occurred in China during the 110 years from 1900 to 2010 accounted for about 2.5% of radiated energy globally, but the earthquake fatality ratio is around 1/3 of the world (Wu et al., 2013). Among the losses caused by natural disasters, buildings are considered as the most important asset category, since the main sources of loss and fatality that occurs during earthquakes are related to building damage and collapse (e.g., Neumayer and Barthel, 2011; Yuan, 2008). Information on the exposed value of buildings is key to seismic loss estimation, whose accuracy will further affect the effectiveness in earthquake response and rescue (Xu et al., 2016a). Therefore, in any seismic risk mitigation effort, the estimation of the building stock and the values at risk should be given top priority. This is even more urgent for seismic active and disaster vulnerable countries like China (Allen et al., 2009), where rapid urbanization has led to a massive increase in both the asset value and population that are exposed to a potential seismic hazard (Hu et al., 2010; Yang and Kohler, 2008).

Modeling seismic loss to buildings requires quantifying their exposure in terms of floor area and monetary value (Paprotny et al., 2020). A series of micro-, meso- and macro-scale approaches have been developed for this purpose. The scale of the method depends not only on the size of the study area but also on the goal of the investigation, the availability of necessary data, time, money, and human resources (Messner and Meyer 2006). For example, micro-scale analyses calculate the asset value based on individual buildings, which requires detailed information on building characteristics (e.g., occupancy, age, structure type, building height, or the number of floors). However, since great efforts and considerable expenses are required to collect such information for each building, micro-scale methods are rarely applicable on a regional or (inter)national level (e.g., Figueiredo and Martina, 2016; Erdik, 2017). When further limited by the privacy protection issue, information on asset values of individual buildings is more difficult to obtain (Wünsch et al., 2009). In contrast, meso- and macro-scale methods that use aggregated exposure data on building characteristics procured from official statistics and organized in administrative units (e.g., country, province, prefecture, county/district, etc.) are more commonly used in modeling building values exposed to future earthquakes.

Since building-related statistics are usually aggregated at a coarse administrative level, while seismic hazards are usually modeled with high spatial resolution, there is a spatial mismatch between exposure data and hazard mapping (e.g., Chen et al., 2004; Thieken et al., 2006). This mismatch may delay and mislead the recuse decision-making after large earthquakes. For example, after the occurrence of the Ms8.0 Wenchuan earthquake, one of the most severely affected areas, Qingchuan County, did not get an appropriate rescue response, while most of the recuse resources were sent to the less damaged Dujiangyan City. The major reason for this problem was: The exposure data (population, buildings) used to assess seismic loss were based on administrative units (Xu et al., 2016). Therefore, to enhance seismic risk assessment accuracy, the aggregated building statistics data need to be

spatialized into high-resolution grids levels. Several interpolation and decomposition methods (e.g., areal weighting, pycnophylactic interpolation, dasymetric mapping) have been developed for this purpose. Compared with the areal weighting method, in which the aggregated building data are evenly distributed (e.g., Goodchild et al. 1993), pycnophylactic interpolation method uses a smoothing function of distance to determine the disaggregation weight (e.g., Tobler, 1979) and tends to be more reasonable, since the distribution of buildings within an administrative unit is heterogeneous. Based on the pycnophylactic interpolation method, the dasymetric mapping method (Bhaduri et al., 2007) further utilizes finer resolution ancillary spatial data to augment the interpolation process and is now widely used.

When using the dasymetric mapping method to spatialize the administrative level building exposure data, the selection of appropriate ancillary information is thought to be the most difficult part (Wu et al., 2018), since such information should not only be geo-coded and readily available but also have a high correlation with the building exposure data to be disaggregated. A range of remote sensing data (e.g., nightlight data, road density, land use/land type, population spatial distribution datasets, etc.) has been employed as ancillary information in the literature. A detailed summary of these ancillary data will be given in the Data Sources and Methodology section.

Based on the aggregated building-related statistics and using the dasymetric mapping method, this paper develops a high-resolution residential building model (in terms of building floor area and replacement value) for seismic risk assessment in mainland China. This issue has been explored in many previous studies and a series of global and regional building exposure models have been developed. One famous such global model is the PAGER (Prompt Assessment of Global Earthquakes for Response) building inventory database, which is the first open, publicly available, transparently developed global model (Jaiswal et al., 2010). However, the PAGER inventory was developed to rapidly estimate human occupancies in different structure types for earthquake fatality assessment. It lacks information in actual building counts and does not use available information from a commercial database or remote sensing data, thus cannot be used for building asset evaluation immediately (Dell'Acqua et al., 2013). To overcome this difficulty, at least partially, the GED4GEM (the Global Exposure Database for the Global Earthquake Model) project develops a complementary approach that can provide a spatial inventory of exposed assets for catastrophe modeling and loss estimation worldwide (Gamba, 2014). The input datasets ingested into the GED4GEM are at multiple spatial scales, from coarse country-level statistics to finer compilations of each building in some sample regions. There are also other global models, such as the series of building stock models released by the Global Assessment Report (De Bono and Chatenous, 2015; De Bono and Mora, 2014; De Bono et al., 2013) of the United Nations International Strategy for Disaster Reduction (UNISDR), and the global exposure dataset created by Gunasekera et al. (2015). When focusing on the modelling of building stock in China, a common limitation shared by these global models is that the building-related statistics they disaggregate are only of country/sub-country level, although finer level statistics are already available. Thus, a general assumption in the disaggregation process of these global models is that building stock value per capita within the country/sub-country is uniform. A similar assumption is also made in studies that develop building exposure models specifically for China (e.g., Yang and Kohler, 2008; Hu et al., 2010). For computational convenience, such an assumption is acceptable. However, for improving the seismic risk assessment accuracy in each specific country, more detailed aggregated data at a finer level, if available, should be fully employed in the development of their building exposure model.

By considering the depreciation of all physical fixed assets (including residential and non-residential buildings, infrastructures, tools, machinery, and equipment), Wu et al. (2014) estimated the wealth capital stock (WKS) value for 344 prefectures in mainland China using the perpetual inventory method (PIM). Later, Wu et al. (2018) decomposed the prefecture-level WKS value into building assets, infrastructure assets, and other assets with fixed percentage shares of 44%, 19%, and 37% for all 344 prefectures. And these three asset components were further disaggregated into 800m×800m high-resolution grids by using LandScan population, road density, and nighttime light as ancillary information, respectively. The basic idea of combining the use of different ancillary information to disaggregate the WKS value in Wu et al. (2018) is good. However, the over-simplification in fixing the percentage shares of the building, infrastructure, and other assets in all prefectures limits the applicability of their results in actual seismic risk assessment.

Based on the county-level building-related statistics extracted from the 2010-census records, Xu et al. (2016b) developed the nation-wide dasymetric foundation data (including population and buildings) for quick earthquake disaster loss assessment and emergency response in China by using the multi-variate regression method (Xu et al., 2016a). The multivariate regression method used in Xu et al. (2016a) was explained in more detail by Chen et al. (2012) and Han et al. (2013), in which they developed the population and building exposure models for areas in Yunnan Province. Fu et al. (2014a) also used the multi-variate regression method to produce the 1km×1km resolution population grids in the years 2005 and 2010 for mainland China. Important assumptions in this multivariate regression method are: (1) The spatial distribution of population is limited within the six land use types (namely cultivated land, forest land, grass land, rural residential land, urban residential land, industrial and transportation land) recognized from the Landsat TM images; (2) For counties with similar geographical and demographic characteristics (e.g., population number, structure and economy development level), the population density within each land use type is the same. Recently, Lin et al. (2020) conducted a township/street level comparison of population models generated by Fu et al. (2014a) and other institutes for Guangdong Province, China with the surveyed population in 2010-census records. Their comparison shows that the township/street level population generated by using the multi-variate regression method in Fu et al. (2014a) tends to overpredict the population density in a sparsely populated area and underpredict the population density in a densely populated area, especially the downtown area of metropolitan cities like Shenzhen and Guangzhou. The reasons for such discrepancies are that: (1) The population density developed for each land use type by using the multi-variate regression method is the average population density, thus the over/under prediction of the actual population density in certain areas is inevitable; (2) When applying the multi-variate regression method, no additional supplementary data (e.g., road density, nighttime light) is employed to adjust the level of development in different regions, which is necessary because the level of development is much higher than the average in places such as the downtown area of metropolitan cities like Shenzhen and Guangzhou. Although the building exposure model developed by Xu et al. (2016b) has not yet been tested, we conclude that the model of Xu et al. (2016b) also suffers from the over/under prediction problem in Fu et al. (2014a).

To overcome the limitations in building exposure models developed for mainland China in previous studies, this paper aims to present an improved method for generating a high-resolution residential building stock model (in terms of building floor area and replacement value) for mainland China. The main improvements in this paper are: (1) Compared with global building exposure models, we will use finer urbanity level (urban, township and rural) building related statistics extracted from the 2010-census records as model inputs; (2) Compared with Wu et al.

(2018), in which the building assets are decomposed from the composite WKS value with fixed percentage share for all prefectures, we will use statistics that are directly related to residential buildings for each urbanity level of each province; (3) Compared with Xu et al. (2016b), in which only land use data are employed in the multi-variate method to derive the average building floor area density within each grid, we will use the ancillary population density profile generated from the 2015 Global Human Settlement Layer (GHSL), which is considered to be the best available assessment of spatial extents of human settlements with unprecedented spatial-temporal coverage and detail (e.g., Freire et al., 2016).

The organization of the paper is as follows. Sect. 2 (Data Sources and Methodology) will firstly describe the building-related statistics to be used as model inputs that extracted from the 2010-census records (Sect. 2.1), the review and selection of ancillary data to disaggregate these statistics into grid level (Sect. 2.2), and the derivation of residential building floor area and replacement value in each grid based on these statistics and the ancillary data (Sect. 2.3 and 2.4). Then the major results will be presented (Sect. 3.1) and comparisons with other independent data sources will be conducted (Sect. 3.2). Limitations in this paper and further improvement directions will also be discussed in Sect. 4. Conclusions will be drawn in Sect. 5.

2.   Data Sources and Methodology

In dasymetric mapping, the use of finer scale census data as input and the choice of appropriate ancillary remote sensing data to disaggregate the census data into a higher grid level are the two controlling factors for the quality of the building stock model. For China, after the 2010 Sixth Population Census (namely the 2010-census), detailed statistical data related to residential building characteristics (e.g., building occupancy, structure type, height classes, etc.) are available for each province at the urbanity level (urban/township/rural). These urbanity level building-related statistics are good data sources to develop the building exposure model for China. To disaggregate these statistics into grid level, the correlation between the ancillary remote sensing data and the building-related statistics needs to be established. Then, the building floor area and replacement value at the grid level can be estimated. Therefore, in this section we will introduce the residential building-related statistics as extracted from the 2010-census records, the review/selection of ancillary remote sensing data to disaggregate these statistics into grid level, and the method to derive the grid level residential building floor area and replacement value based on these statistics and the ancillary remote sensing data.

2.1 The building-related statistics in the 2010-census records

The statistics to be used in this paper for building stock modeling are extracted from the Tabulation of the 2010 Population Census of the People's Republic of China (namely the 2010-census) particularly for residential buildings. Like in most countries of the world, the nation-wide population and housing census in China are carried out at the 10-year interval. Detailed statistics for the year 2020 are not publicly accessible yet. Therefore, census data for the year 2010 will be used to elaborate the modeling process. In the 2010-census, there are two types of tables: Long Table and Short Table. Long Table includes summaries based on the surveys of 10% of the total population in mainland China, while the Short Table summaries are based on the surveys of the whole population. Statistics on building characteristics (e.g., building occupancy type, height classes, structure type, etc.) are extracted from the Long Table of the 2010-census. Supplementary demographic statistics (e.g., the total population

190   in each urbanity, the average number of people per family, and average floor area per person) are extracted from the Short Table of the 2010-census. A detailed introduction of corresponding sources of these data is given in Table 1.

For each of the 31 provincial administrative units in mainland China (including five autonomous regions: Xinjiang, Tibet, Ningxia, Inner Mongolia, Guangxi; and four municipalities: Beijing, Shanghai, Tianjin, Chongqing;

195   hereafter all referred to as provinces), statistics on building characteristics in the Long Table of the 2010-census are aggregated into three urbanity levels (urban/township/rural). The urbanity attribute is determined according to the administrative unit of the surveyed population. As listed in Table 2, these statistics will be used as model inputs to develop the grid level residential building model in terms of floor area and replacement value. Compared with country/sub-country level census data used in previous global or regional models, the further categorization of

200   building-related statistics into urbanity level in the 2010-census helps differentiate the spatial heterogeneity of buildings within each province, since the building-related statistics of the same urbanity level are from areas with similar development background but different administrative units. The spatial administrative boundaries used in this paper are from the National Geomatics Centre of China (see Data/Code Availability section for access).

2.2 Review/Selection of ancillary remote sensing data for dasymetric building stock modeling

205   Before disaggregating the urbanity level building-related statistics into 1km×1km grid level, appropriate ancillary information needs to be carefully selected and evaluated. The use of remote sensing data as ancillary information to determine the disaggregation weight is common in dasymetric modeling and has been frequently adopted in previous studies (e.g., Aubrecht et al. 2013; Gunasekera et al., 2015; Silva et al., 2015). The most commonly used remote sensing data include land use/land cover data (LULC, e.g., Eicher and Brewer, 2001; Wünsch et al., 2009;

210   Seifert et al., 2010; Thieken et al., 2006), nighttime light data (e.g., Doll et al 2006; Ghosh et al, 2010; Chen and Nordhaus 2011; Ma et al., 2012) and road density data (e.g., Gunasekera et al., 2015; Wu et al., 2018). According to Wu et al. (2018), the LULC, nighttime light, road density data can be categorized as primary remote sensing data.

Each primary remote sensing data has its pros and cons when used for dasymetric disaggregation. For example,

215   studies using LULC data (e.g., Globcover, GLC2000, MODIS, GlobeLand30) assume the population within each land-use type is uniformly distributed, which is a better assumption compared with believing in an evenly distributed population within an administrative unit. But this assumption is not consistent with the real situation. (Thieken et al., 2006), specifically in suburban and rural areas, where the dispersion of population is greater than in urban areas (Bhaduri et al., 2007). Therefore, LULC data is inadequate to fully reflect the spatial heterogeneity

220   within each land use or land cover class. In contrast, nighttime light data, acquired by the U.S. Air Force Defense Meteorological Satellite Program (DMSP) Operational Linescan System (OLS) (Elvidge et al., 2007) and provided by the National Oceanic and Atmospheric Administration (NOAA) every year, are considered the most suitable ancillary information for indicating both the distribution and the density of human settlements and economic activities (Wu et al., 2018). Nighttime light data have been widely used to produce grid-based global population

225   and GDP data sets (e.g., Ghosh et al 2010; Chen and Nordhaus 2011; Ma et al., 2012). However, the drawbacks of nighttime light intensity data are also obvious. Limited by the operating conditions of DMSP satellites, the range of nighttime light density is within a narrow interval of 0-63, thus leading to the pixel oversaturation in urban

centers (Elvidge et al., 2007). For areas other than city centers (e.g., mountainous rural area), the coverage of nighttime light data is incomplete as it cannot correctly reflect the distribution of nonluminous objects (e.g., road transportation facilities, electricity infrastructure). Compared with the LULC and nighttime light data, road distribution data are more frequently used for assessing infrastructure assets, since power lines, energy pipelines, water supply, and sewage pipelines are generally buried along the roads (Wu et al., 2018). Currently, road density data can be converted from road networks like OpenStreetMap, which is an openly available but crowdsourced online database (Zhang et al., 2015). As these data are not systematically compiled, there is still room for improvements (Wu et al., 2018).

Given the limitation of each primary remote sensing data, a series of secondary ancillary datasets are developed based on the combined use of these primary datasets. For example, the famous LandScan population density profile was produced by apportioning the best available census counts into cells based on probability coefficients, which were derived from road proximity, slope, land cover, and night-time lights (Dobson et al., 2000). Based on these primary and secondary ancillary datasets, a series of studies have been conducted to disaggregate administrative level building census data into geo-coded grids. For example, Silva et al. (2015) disaggregated the building stock at parish level for mainland Portugal based on the population density profile at 30×30 arc-sec resolution cells from LandScan. Gunasekara et al. (2015) developed an adaptive global exposure model (including three independent geo-referenced databases, namely building inventory stock, non-building infrastructure, and sector-based GDP), in which build-up area and LandScan population density are used to disaggregate country-level exposed asset value. Wu et al. (2018) established a high-resolution asset value map for mainland China by spatializing the prefecture-level depreciated capital stock value into girds using the combination of three ancillary datasets— nighttime light, LandScan population, and road density, to name just a few.

In this paper, we follow the assumption of Thieken et al. (2006) that the distribution of residential asset values can be directly reflected by population distribution. Now the remaining question is to select appropriate ancillary population spatial distribution data to disaggregate building-related statistics in the 2010-census records. The candidate population datasets include Gridded Population of the World (GPW, Balk and Yetman, 2004), Global Rural-Urban Mapping Project (GRUMP) population (see section Data/Code Availability), LandScan (Bhaduri et al., 2007), WorldPop (Linard et al., 2012) or AsiaPop (Gaughan et al., 2013), PopGrid China (Fu et al., 2014b), Global Human Settlement Layer (GHSL) population grids (Freire et al., 2016; Pesaresi et al., 2013) etc. GPW is a product of simple areal weighting interpolation and GRUMP is derived through simple dasymetric modeling, while LandScan is structurally a multidimensional dasymetric model (Bhaduri et al., 2007). According to Gunasekera et al. (2015), the LandScan gridded population dataset was identified as the best-suited dataset for exposure disaggregation, while other gridded population datasets such as GPW and GRUMP were too coarse in resolution and accuracy. According to Wu et al. (2018), LandScan, AsiaPop, and PopGrid China are the most promising population density datasets for asset value disaggregation in China since they all contain high-resolution attributes. However, some population data of China are missing from the current AsiaPop. And compared with LandScan, the spatial coverage of PopGrid China is limited, which is due to an assumption in its development method, namely the multi-variate regression method (Fu et al., 2014a). It was assumed that the spatial distribution of population is limited to the six land use types recognized from the Landsat TM images, namely cultivated land, forest land, grass land, rural residential land, urban residential land, industrial and transportation land. However, in reality, the population is distributed more widely beyond these land use types. Thus, the LandScan dataset was used for the

final disaggregation of building assets in Gunasekera et al. (2015) and Wu et al. (2018). However, due to its commercial nature, the details to create the LandScan population datasets are less transparent, although being considered as one of the best global population density data sets (Sabesan et al., 2007). In contrast, the population datasets developed by the GHSL project of Joint Research Center of the European Commission based on the global human settlement areas extracted from multi-scale textures and morphological features are transparent and freely available. The built-up area in GHSL was built by combining the MODIS 500 Urban Land Cover (MODIS500) and the LandScan 2010 population layer and are among the best-known binary products based on remote sensing (Ji et al., 2020). Preliminary tests confirm that the quality of the information on built-up areas delivered by GHSL is better than other available global information layers extracted by automatic processing of Earth observation data (Lu et al., 2013; Pesaresi et al., 2016). Furthermore, Different from LandScan, which aims at representing the ambient population, namely the average population over a typical diurnal cycle (Elvidge et al., 2007), GHSL population grids represent the residential population in buildings (Corbane et al., 2017). The building-related statistics in the 2010-census are also for residential buildings. Therefore, the GHSL population grids are the best candidate ancillary information for this paper to disaggregate the urbanity level building-related statistics extracted from the 2010-census records into grid level. The high correlation ($R^2 = 0.9662$, as shown in Fig. 1) between the GHSL population and the 2010-census recorded population at the county-level further indicates its appropriateness. Detailed county-level population correlation analyses for each of the 31 provinces in mainland China are also provided and can be found from the online supplement. The accesses to the remote sensing data mentioned above are provided in the Data/Code Availability section.

2.3 Assign urbanity attribute (urban/township/rural) to the geo-coded grids in the 2015 GHSL population density profile

In the 2015 GHSL population density profile, the number of populations in each geo-coded grid is given (it is worth noting that this dataset has been updated in 2019 during the preparation of this work). The original resolution of the 2015 GHSL population density profile is 250m×250m. For computational convenience, it is resampled to 1km×1km resolution before further analysis. Based on the urbanity level residential building-related statistics extracted from the 2010-census records, a top-down dasymetric mapping method will be performed to disaggregate the urbanity level statistics into 1km×1km resolution grids for mainland China. The urbanity attribute of statistics in the 2010-census records is determined according to the administrative unit of the surveyed population. For example, if a residence is from a village, then the related statistics are aggregated into rural urbanity level; and if from a town, then it is township level; if from a city, it is urban level. However, for the geo-coded population grids in the 2015 GHSL profile, the corresponding urbanity attributes remain to be defined. Therefore, before performing the disaggregation, we will first define the urbanity attribute of each geo-coded grid in the 2015 GHSL profile by applying the reallocation approach developed by Aubrecht and Leon Torres (2015) and illustrated in Gunasekera et al. (2015).

Aubrecht and Leon Torres (2015) identify the geospatial areas of mixed and residential grids within the urban extent of Cuenca City, Ecuador by using the Impervious Surface Area (ISA) data as they show strong spatial correlations with the built-up areas. The assumption behind their method was that intense lighting is associated with a high likelihood of commercial and/or industrial presence (which is commonly clustered in certain parts of a city, such as central business districts and/or peripheral commercial zones, and such areas are defined as "mixed-

8

use area"), and areas of low light intensity are more likely to be pure residence zone (defined as "residential use area"). In Gunasekera et al. (2015), a similar procedure was used in developing the building stock model for the entire globe. The difference is that Gunasekera et al. (2015) sorted the grids according to the population density in the LandScan population dataset and assigned the gird with urban/rural attributes. For each country, the largest and most populated contiguous grids are classified as urban. This step was repeated iteratively until the urban population proportion for each country was reached.

In this paper, to assign the urbanity attributes (namely urban/township/rural) to geo-coded population grids in the 2015 GHSL profile, for each province we follow the urban/township/rural population proportions (as listed in Table 3) derived from the population statistics in the Short Table of the 2010-census. The assumption behind this urbanity attribute assignment practice is that the larger the population density in a grid, the higher its potential to be assigned as "urban". An example demonstrating the distribution of the 2015 GHSL population grids assigned with urban/township/rural attributes for Baoshan District of Shanghai is shown in Fig. 2. For instance, in Shanghai, the urban/township/rural population proportion derived from the 2010-census records is 76.64%, 12.66%, and 10.7%, respectively. Then, following Gunasekera et al. (2015), the grids (1km×1km) in the 2015 GHSL profile of Shanghai are sorted from the largest to the smallest in population density. The population in those most populated grids are selected and summed up until the urban population proportion (i.e., 76.64% for Shanghai) is reached. Then those selected grids are assigned with the "urban" attribute and the smallest population among these grids determines the threshold to divide urban and non-urban grids (for Shanghai this urban/non-urban grid population threshold is **4936** per km^2). For the remaining non-urban grids, the same process is repeated iteratively until the township population proportion (i.e., 12.66% for Shanghai) is reached. These grids are assigned with the "township" attribute and the smallest population among these grids determines the threshold to divide township and rural grids (for Shanghai this township/rural grid population threshold is **2750** per km^2). The remaining grids are thus assigned with the "rural" attribute. The urban/township and township/rural population thresholds for 31 provinces in mainland China are listed in Table 3. This process is repeated for all provinces.

2.4 Residential building stock modeling process

The following section will introduce the key steps in residential building stock modeling, including the disaggregation of urbanity level statistics extracted from the 2010-census records into grid level, the reclassification of building subtypes with both structure type and storey class, the derivation of residential building floor area and replacement value in each grid. The flowchart in Fig. 3 gives an overview of the whole modeling process.

2.4.1 Step 1 - Disaggregate urbanity level building-related statistics from the 2010-census into grid level

Like in many other countries, the population and housing census data in mainland China are particularly surveyed for residential buildings. Therefore, the building stock model developed in this paper is for residential building stock. As listed in Table 2, building-related statistics extracted from the 2010-census records include the number of families living in buildings grouped either by the number of the storey (i.e., 1, 2-3, 4-6, 7-9, ≥10) or by structure type (i.e., steel/reinforced-concrete, mixed, brick/wood, other; hereafter steel/reinforced-concrete is abbreviated as steel/RC; and "mixed" refer to different combinations of masonry buildings), the average population per family and the average floor area per capita. For each urbanity level of each province, **the number of families** living in

buildings grouped by storey number or structure type is extracted from the Long Table of the 2010-census, which is based on the survey of only 10% of the total population in mainland China (as noted in Table 1). Therefore, the number of families living in different building types needs to be extended from 10% to 100% population first. This is achieved directly by multiplying the number of families with the factor of 10 (namely factor $F0$ in Step 1-1 of Fig. 3). Multiplying the number of families with the average number of population per family (namely factor $F1$ in Step 1-2 of Fig. 3, with values listed in Table 2) provides **the number of populations** living in buildings grouped by storey number (1, 2-3, 4-6, 7-9, ≥10) or structure type (steel/RC, mixed, other, brick/wood) for each urbanity of each province.

The geo-coded population grids in the 2015 GHSL profile with assigned urbanity attributes (Sect. 2.3) and the number of populations living in buildings grouped by storey number or structure type derived for each urbanity of each province seem to allow the direct disaggregation of the 2010-census statistics into the 2015 GHSL grids. However, the GHSL population is for the year 2015, while the derived population living in different structure type or storey class from the building-related statistics is for the year 2010. The increase in population/building from 2010 to 2015 must be considered. Here we assume that the increase in population living in buildings grouped by storey class or structure type from 2010 to 2015 is equal to the increase in population from the 2010-census records to the 2015 GHSL profile. Therefore, for each urbanity of each province, the derived number of populations living in building types grouped by storey class or structure type (after performing Step 1-1 and 1-2 in Fig. 3) will be further amplified to the year 2015 by multiplying the population amplification factor (namely factor $F2$ in Step 1-3 of Fig. 3). For each urbanity of each province, the value of $F2$ is equal to the ratio of the 2015 GHSL population to the sum of the population living in buildings of different occupancy types. For example, in urbanity "1001" of Anhui province in Table 2, the value of $F2$ (1.32) results from the ratio of the 2015 GHSL population (12165295) to the product of the number of families living in three occupancy types (331730+9035+287 = 341052; based on surveys of 10% of the whole population), the average number of population per family ($F1$ = 2.71), and the factor to extend the 10% population survey to 100% population ($F0$ = 10), namely 12165295 / (341052×2.71×10) = 1.32.

Thus, for each urbanity of each province, the number of populations living in buildings grouped by storey class or structure type in 2015 is derived by multiplying the original number of families living in different building types (based on surveys of 10% of the whole population) in Table 2 with factor $F0$, $F1$, $F2$. These urbanity level statistics can be disaggregated into the geo-coded grids of the 2015 GHSL profile. The population share in each grid (relative to the sum of population of grids with the same urbanity) is used as the disaggregation weight (namely factor $F3$ in Step 1-4 of Fig. 3). By multiplying the urbanity level population living in buildings grouped by storey class or structure type with the disaggregation factor $F3$ of each grid, the grid level number of populations living in buildings grouped by storey class or structure type can be directly derived.

2.4.2 Step 2 - Derive the population living in the 17 building subtypes within each grid

As explained in Section 2.4.1, after multiplying the original number of families living in different building types extracted from the 2010-census records (Table 2, based on surveys of 10% of the whole population) with factor $F0$, $F1$, $F2$, and $F3$ in Step 1 of Fig. 3, the grid level populations living in buildings grouped either by the number of storey (1, 2-3, 4-6, 7-9, ≥10) or by structure type (steel/RC, mixed, other, brick/wood) are derived for all geo-

coded grids in the 2015 year level. To further estimate the residential building floor area and replacement value in each grid, we need to evaluate the unit construction prices of the building types in each grid. Currently, the building types are grouped either by storey number or by structure type, and they need to be reclassified into building subtypes with both storey class and structure type attributes. Then it will be easier and more reasonable to estimate the unit construction prices of these building subtypes, compared to the estimation made in studies based on building occupancy type (e.g., Wu et al., 2019).

In the following description, we will first introduce the reclassification of building subtypes with both storey class and structure type attributes. Then we will estimate the population living in each of the 17 building subtypes. Based on the statistics of average floor area per capita in each urbanity level extracted from the 2010-census records (as listed in Table 2), the total floor area of each of the 17 building subtypes in each grid can be derived. Finally, for each building subtype, their replacement value emerges from a multiplication of the floor area with the unit construction price.

By combining the five storey classes (1, 2-3, 4-6, 7-9, ≥10) with the four structure types (steel/RC, mixed, other, brick/wood), the building types in the 2010-census records can be initially reclassified into 20 building subtypes. According to Hu et al. (2015) and Wang et al. (2018), most brick/wood buildings are with quite low height (1 or 2-3 storey), while steel/RC buildings are generally quite high with 10-storey height and above. Therefore, in this paper it is assumed that for "brick/wood" structure type, there are only two storey classes (1, 2-3); while for "steel/RC", "mixed", and "other" structure types, all five storey classes (1, 2-3, 4-6, 7-9, ≥10) are available (namely the assumptions in Step 2-1 and 2-2 of Fig. 3). Thus, the number of building subtypes with known storey class and structure type is reduced from 20 to 17. The abbreviations of these 17 building subtypes are listed in Table 4.

After performing the calculations in Step 1 of Fig. 3, the grid level populations living in buildings grouped either by the number of storey (1, 2-3, 4-6, 7-9, ≥10) or by structure type (steel/RC, mixed, other, brick/wood) are derived for all geo-coded grids. Thus, we know in each grid the number of population living in buildings of the five storey classes, but we do not know for each storey class how the population is distributed among the four structure types. Also, we know how many people live in steel/RC buildings or other structure types, but for each structure type, we do not know how they are distributed into the five storey classes. For each grid, to derive the number of population living in each of the 17 building subtypes with known structure type and storey class, we need to solve 17 unknown variables from 9 equations. The 9 equations are listed as follows:

$$BRIWOMC1 + STLRCMC1 + MIXEDMC1 + OTHERMC1 = Num_{storey1} \quad (1)$$
$$BRIWOMC23 + STLRCMC23 + MIXEDMC23 + OTHERMC23 = Num_{storey23} \quad (2)$$
$$STLRCMC46 + MIXEDMC46 + OTHERMC46 = Num_{storey46} \quad (3)$$
$$STLRCMC79 + MIXEDMC79 + OTHERMC79 = Num_{storey79} \quad (4)$$
$$STLRCMC10 + MIXEDMC10 + OTHERMC10 = Num_{storey10} \quad (5)$$
$$BRIWOMC1 + BRIWOMC23 = Num_{BRIWO} \quad (6)$$
$$STLRCMC1 + STLRCMC23 + STLRCMC46 + STLRCMC79 + STLRCMC10 = Num_{STLRC} \quad (7)$$
$$MIXEDMC1 + MIXEDMC23 + MIXEDMC46 + MIXEDMC79 + MIXEDMC10 = Num_{MIXED} \quad (8)$$
$$OTHERMC1 + OTHERMC23 + OTHERMC46 + OTHERMC79 + OTHERMC10 = Num_{OTHER} \quad (9)$$

The 17 to-be-solved variables on the left side of this equation set represent the numbers of populations living in the 17 buildings subtypes (as defined in Table 4); on the right side, the numbers are populations living in buildings classified by fives storey class and four structure types, which are already known after performing the calculations

in Step 1 of Fig. 3. Since this set of 9 equations contains 17 unknown variables, it is an underdetermined linear problem. In order to provide values for the 17 unknowns, additional assumptions have to be utilized.

The strategy we employ here to derive the population living in each of the 17 building subtypes of each grid is a series of distribution steps based on a prioritized ranking of building types and storey classes. For example, we first assign 1 storey class buildings into brick/wood structure type and distribute ≥10-storey class as steel/RC structure type (following the assumptions in Step 2-1 and 2-2 of Fig. 3). Although this distribution strategy may deviate from the actual situation, the basic requirement, that in each grid the sum of the population living in the 17 building subtypes is equal to the population living in building types grouped by structure type or by storey class, is satisfied. The main distribution steps are summarized in Appendix A.

2.4.3 Step 3 - Derive the residential floor area of the 17 residential building subtypes in each grid

Based on the distribution processes in Appendix A, we derive the number of populations living in each of the 17 building subtypes in each gird. To derive the residential floor area of each building subtype, the average residential floor area per capita is needed, which is given in the Short Table of 2010-census (namely factor $F4$ in Step 3-1 of Fig. 3) for each urbanity level of each province. Therefore, the floor area of the 17 building subtypes in each grid can be directly derived. This grid level residential building floor area distribution map is available from the online supplement. Comparison between the modeled floor area and the 2010-census recorded floor area for residential buildings at county/district-level will be performed in Sect. 3.2.2.

2.4.4 Step 4 - Derive the replacement value of the 17 residential building subtypes in each grid

With the residential building floor area for each building subtype in each grid being derived in Step 3, to get the corresponding replacement value, the unit construction prices of the 17 building subtypes need to be estimated (namely factor $F5$ in Step 4-1 of Fig. 3). Given the uniqueness of the building reclassification strategy adopted in this paper, there are no standard unit construction price evaluations for the building subtypes we use here. Therefore, we estimate the unit construction prices of the 17 building subtypes (as listed in Table 4) by averaging the construction prices given in different literature (e.g., 2015 China Construction Statistical Yearbook, the World Housing Encyclopedia, real-estate agency reports, etc.). For the 17 building subtypes in each grid, by multiplying their floor area with the corresponding unit construction price in Table 4, their replacement values can be directly derived. This grid level residential building replacement value distribution map is also available from the online supplement. We emphasize that in this paper, the term "replacement value" refers to the amount of money needed to rebuild a property exactly as it is before its destruction regardless of any depreciation, namely the gross capital stock. A prefecture-level comparison between our modeled residential building replacement value and the wealth capital stock value in Wu et al. (2014) will be given in Sect. 3.2.1.

12

3. Results and Performance Evaluation

455 **3.1 Results**

3.1.1 Modeled floor area and replacement value for residential buildings in each urbanity of each province

The grid level residential building floor area and replacement value (unit: RMB, in 2015 current price) are aggregated into urbanity level (urban/township/rural) for each province, as listed in Table 5. The total modeled residential building floor area for mainland China in 2015 reaches 42.31 billion m^2. By applying the same unit

460 construction prices for the same 17 building subtypes in all the urban/township/rural areas of the 31 provinces, the initially modeled replacement value of residential buildings in mainland China is 77.8 trillion RMB (in 2015 current price). It is clear that like all other building stocks, the Chinese building stock is a complicated economic, physical and social system (Yang and Kohler, 2008). There are significant differences across the country in terms of economic development level, geographic and climatic diversity, and standardization in building construction.

465 Therefore, it is mainly for computational convenience that this paper applies the same unit construction price for all the provinces and all the urbanity levels. To improve accuracy in future seismic risk assessment, the unit construction prices of specific building types in the target study area should be adjusted accordingly.

3.1.2 An example illustrating the distribution of modeled floor area in Shanghai

For better visualization of the modeled floor area at grid level and to help potential readers to conduct direct

470 comparison with other reports or modeling results, we plot the residential building floor area distribution map and the 2015 GHSL population of Shanghai as an example. As can be seen from Fig. 4, grids with a high density of floor area typically cluster in the downtown area (including eight administrative districts, namely Yangpu, Hongkou, Zhabei, Putuo, Changning, Xuhui, Jing'an, and Huangpu) and the Pudong district. This corresponds to the fact that these districts are the most developed in Shanghai.

475 **3.2 Performance Evaluation**

As of now, we have developed a high-resolution (1km×1km) residential building stock model (in terms of floor area and replacement value) for mainland China. This model is established by disaggregating the urbanity level building-related statistics in 2010-census records into grid level and using the 2015 GHSL geo-coded population as the disaggregation weight. Due to the approximations and assumptions made in the modeling process, the

480 reasonability and consistency of the modeled results need to be evaluated. Due to the typical lack of official statistics on high-resolution building stock from the government (Wu et al., 2018), direct comparison of the modeled floor area and replacement value at grid level with that from official census or statistical yearbooks are not instantly available. Instead, we will compare our modeled results with other studies or census records at a coarser level. Moreover, since the development of such a high-resolution residential building model is mainly

485 targeted for seismic risk assessment in mainland China, we will also apply our modeled results to seismic loss estimation combining with the 2008 Wenchuan Ms8.0 earthquake intensity map and an empirical loss function. The estimated losses will be compared with those recorded in affected counties/districts of Sichuan Province.

3.2.1 Prefecture-level comparison between the modeled residential building replacement value and the net capital stock value estimated in Wu et al. (2014)

490   Due to the lack of officially published datasets on the value of fixed capital stock in China (Wu et al., 2018), previous studies (e.g., Holz, 2006; Wang and Szirmai, 2012) mainly employed the perpetual inventory method (PIM) in which economic indicators (e.g., gross fixed capital formation, total investment in fixed assets, etc.) are used. The resolutions of these estimations were almost exclusively limited at national/provincial-level (Wu et al., 2014). This coarse spatial resolution forms a major obstacle in applying the model in disaster loss estimation,

495   where high-resolution hazard data are used. To overcome this gap, Wu et al., (2014) estimated the net capital stock values from 1978 to 2012 for 344 prefectures in mainland China by using the PIM. In their Appendix Table A1, the net capital stock values calculated in 2012 current price for 344 prefectures were provided, with the depreciation of all exposed assets (i.e., residential and non-residential building structures, tools, machinery, equipment, and infrastructure) being considered.

500   To compare with the net capital stock value in Wu et al. (2014), the grid level residential building replacement value modeled in this paper (namely the gross value of residential building stock) was aggregated into prefecture-level. Pearson's correlation coefficient (R^2) was used to measure the degree of collinearity between two datasets, with higher R^2 indicating a stronger correlation. As shown in Fig. 5, there is a high correlation ($R^2 = 0.9512$) between our residential building replacement values and the net capital stock values in Wu et al. (2014) at the

505   prefecture-level. The absolute replacement value of residential buildings is around 0.54 times the net capital stock value in Wu et al. (2014). To explain this discrepancy, we collected the annual fixed asset investment on residential buildings and on all types of buildings for each of the 31 provinces during the years 2004-2014 from the statistical yearbooks (detailed statistics are available from the online supplement). As can be seen from Fig. 6, for each province the sum of fixed asset investment on residential buildings during 2004-2014 is around 0.45 times the

510   investment on all types of buildings, quite close to the 0.54 ratio in Fig. 5. The replacement value we estimate is purely for residential buildings without depreciation, while the net capital stock value in Wu et al. (2014) includes depreciation of all exposed assets (residential, non-residential buildings, infrastructures, and equipment). Thus, we consider our model results as reasonable.

3.2.2 County/prefecture-level comparison between modeled residential building floor area and records in

515   **the 2010-census**

Compared with previous studies related to building stock modeling in China, we have used finer urbanity level building-related statistics as input to generate the grid level residential building stock model. In each urbanity, the building-related statistics extracted from the 2010-census records are from areas with a similar development background, but they belong to different administrative units (i.e., prefectures and counties). Also, within the same

520   prefecture or county, the geo-coded grids are of different urbanity attributes. Therefore, the reliability of our model can be better proved if the modeled results correlate well with actual records at the county or prefecture-level. After a thorough search, we find that county-level records of residential building floor area are also available for 28 provinces in mainland China, except for Hunan, Liaoning, and Sichuan provinces, for which only prefecture-level records of residential building floor area can be found from the 2010-census records. Then, to compare our

525   modeled floor area with the 2010-census records at the county/prefecture-level, the modelled grid level residential

14

building floor area was first aggregated into counties/districts for the 28 provinces, and prefectures for Hunan, Liaoning, and Sichuan, respectively. The final comparison between our estimated residential building floor area with that recorded in the 2010-census is plotted in Fig. 7.

As can be seen from Fig. 7, there is a high correlation ($R^2 = 0.9376$) between modeled floor area and that recorded in the 2010-census at the county/prefecture-level. The regression relation indicates that our modeled floor area for 2015 is around 1.14 times that in the 2010-census. In Step 1-3 of the modeling process (Fig. 3), for each urbanity level of each province, the building-related statistics extracted from the 2010-census records were amplified into the 2015 level by multiplying the factor $F2$. Mathematically speaking, $F2$ is the ratio of the 2015 GHSL population to the 2010-census recorded population. $F2$ is 1.13 for the whole mainland China, which can be derived by following the derivation process of $F2$ illustrated in Sect. 2.4.1 based on the statistics in Table 2. Therefore, we consider the ratio of 1.14 between our modeled floor area for 2015 and that recorded in the 2010-census at the county/prefecture-level as quite reasonable. For each province, we also plotted the correlation analyses for the population (between the 2015 GHSL population and 2010-census recorded population) and for the residential building floor area (between the modeled floor area and the 2010-census recorded floor area), which are available from the online supplement. The corresponding regression parameters and correlation coefficients for the population and the residential building floor area of each province are listed in Table 6.

From Table 6 we can see that the correlation between the 2015 GHSL population and the 2010-census recorded population, and the correlation between the modeled floor area and the 2010-census recorded floor area are generally very high for a majority of provinces (with $R^2 \geqslant 0.9$). This indicates the plausibility of choosing the 2015 GHSL population as the ancillary information to disaggregate the urbanity level building-related statistics, and the reliability of our modeled floor area at the county/prefecture-level. However, it is also worth noting that for coastal provinces like Fujian and Jiangsu, the correlation coefficients of floor area are lower (with $R^2 < 0.82$). We explain this discrepancy with an overpredicted population in the 2015 GHSL profile for the capital or the most developed cities in these provinces (as can be checked from the population correlation analyses for these provinces from the online supplement). Many people tend to work in the capital or the most developed cities without being officially registered as residents. These people are not counted in the 2010-census of these cities but are included in the 2015 GHSL population density profile, which is derived from remote sensing data combined with the actual population density.

3.2.3 Application of the residential building stock model to seismic loss estimation

Since the residential building model developed in this paper is targeted for seismic risk analysis, we now use the modeled replacement value to estimate the seismic loss to residential buildings in Sichuan province caused by the Wenchuan Ms8.0 earthquake. The hazard component used for this loss estimation is the macro-seismic intensity map of the 2008 Wenchuan Ms8.0 earthquake (Fig. 8), which was issued by the China Earthquake Administration (CEA) based on post-earthquake field investigations. The vulnerability function used was the empirical loss function developed in Daniell (2014, Page 242) for mainland China, which provides the relation between macro-seismic intensity and loss ratio (the ratio between repairment cost and replacement cost of buildings damaged in an earthquake). This empirical vulnerability function was developed based on reported seismic damage and loss related to earthquakes that occurred in mainland China in the past few decades. Such information was retrieved

15

through an extensive collection of damage and loss records from journals, books, reports, conference proceedings, and even newspapers.

Our estimated seismic loss of residential buildings in Sichuan province due to the Wenchuan Ms8.0 earthquake is around 432 billion RMB (in 2015 current price). The spatial distribution of loss ratios, i.e., the ratio of the estimated loss to the total residential building replacement value in counties/districts of Sichuan province, is shown in Fig. 9. In other reports and studies on the loss assessment of the Wenchuan earthquake, e.g., in Yuan (2008), the estimated loss to residential buildings in Sichuan province was around 170 billion RMB (in 2008 current price). The officially issued loss estimated by the Expert Panel of Earthquake Resistance and Disaster Relief (EPERDR, 2008) to residential buildings in Sichuan province was around 98.3-435.4 billion RMB, with the median loss around 212.32-247.25 billion RMB (in 2008 current price). It should be noted that in these studies, the unit construction price used for rural/urban/township building replacement was around 800-1500 RMB per m^2, which is 1/2.5-1/1.5 of the unit construction price used in this paper as listed in Table 4. Dividing our estimated loss by the factor of 1.5-2.5, then the difference in construction price used in this paper and previous studies are eliminated, and the estimated loss based on our building exposure model turns from 432 billion to around 144-288 billion RMB (in 2015 current price), which is now consistent with that estimated by EPERDR and Yuan (2008). This simple test further indicates the applicability of our model in seismic loss estimation. Thus, the grid level residential building floor area and replacement value developed in this paper can be regarded as reliable exposure inputs for future seismic risk assessment in mainland China.

4.   Limitations in the model and directions for future improvement

According to studies on assessing the resolution of exposure data required for different types of natural hazards (e.g., Chen et al., 2004; Thieken et al., 2006; Bal et al., 2010; Figueiredo and Martina, 2016; Röthlisberger et al., 2018; Dabbeek et al., 2021), the 1km×1km residential building stock model developed in this paper is sufficient for seismic risk assessment. However, limitations in our model are inevitable due to the assumptions and approximations employed in the modeling process. For example, when disaggregating the urbanity level building-related statistics in the 2010-census into grid level and scaling these statistics from 2010 to 2015, we assume that the number of residential buildings in each grid is proportional to its population weight and the increase in building-related statistics of each urbanity is equal to its population increase, which needs to be carefully evaluated by the local development of building stock (e.g., Fuchs et al., 2015). Secondly, to derive the population living in each of the 17 building subtypes in each grid, we assume that brick/wood buildings are limited to 1 and 2-3 storey classes and distribute the number of steel/RC buildings to ≥10-storey class first, which may not be fully consistent with the real cases. Furthermore, we use the same unit construction prices for the same building subtypes regardless of their variation across province and urbanity, which also needs certain readjustment when applying our modeled residential building replacement value into actual seismic risk analyses.

In the future, with the increasing availability of open source datasets that track individual building features in detail, the current limitations in this paper can possibly be overcome. Attempts have been made to combine publicly available building vector data (which contains the spatial location, footprint, and height of each building) and census records to improve the exposure estimation (e.g., Figueiredo and Martina, 2016, Wu et al., 2019, Paprotny et al., 2020). Algorithms to extract building footprints and height from aerial imagery and using computer vision

16

techniques have been used by commercial companies like Google and Microsoft (Parikh, 2012; Bing Maps Team, 2014). More recently, by using an unmanned aerial vehicle and a convolutional neural network, Xiong et al. (2020) introduced an automated building seismic damage assessment method, in which not only the 3D building structure can be constructed, but also the building damage state can be predicted automatically with an accuracy of 89%. In addition, Li et al. (2020) developed the first continental-scale dataset on 3D building structure (including building footprint, height, and volume) at 1km×1km resolution for Europe, China, and the US by using random forest models fed with remote sensing and Synthetic Aperture Radar imagery data. Liu et al. (2021) developed the urban floor area map for mainland China at 130m×130m resolution based on high spatial resolution nighttime light LUOJIA 1-01 images, a population map and a single building dataset encompassing 71 cities. Ji et al. (2020) generated the 10m×10m resolution model of rural settlements in the Yangtze River Delta of China by using the multi-source remote sensing datasets with the Google Earth Engine Platform. Cao and Huang (2021) proposed a multi-spectral, multi-view, and multi-task deep network (called M³Net) for building height estimation. They estimated the building height at a spatial resolution of 2.5m×2.5m for 42 Chinese cities. Comparison with the results in Li et al. (2020) indicated that the M³Net method in Cao and Huang (2021) can better alleviate the saturation effect of high-rise building height estimation than the random forest method used in Li et al. (2020). We take these attempts as an indicator that the high-resolution modeling of building stock for individual buildings will become more widely available in the future.

5. Conclusion

In this paper, a 1km×1km resolution residential building stock model (in terms of floor area and replacement value) targeted for seismic risk analysis for mainland China is developed, by using the 2015 GHSL population density profile as the bridge and by disaggregating the finer urbanity level 2010-census records into grid level for each province. In each grid, a building distribution strategy is adopted to derive the number of population living in each of the 17 building subtypes with structure type and storey class attributes, based on which the floor area and replacement value of each building subtype are derived. In each urbanity of each province, the building-related statistics extracted from the 2010-census records are from areas with a similar development background but different administrative units (i.e., prefectures and counties). Therefore, to evaluate the model performance, the residential building replacement value is first compared with the net capital stock value estimated in Wu et al. (2014) at the prefecture-level. These two datasets are well correlated, and the former is around 0.45 of the latter, which is quite reasonable referring to the fact that for each province the sum of fixed asset investment value on residential buildings is around 0.54 of the sum of investment values on all types of buildings during 2004-2014. Furthermore, county/prefecture-level comparisons of the residential floor area modeled in this paper with records from the 2010-census are also conducted. It turns out that the modeled and recorded residential building floor areas are highly compatible for many counties and prefectures. To further check the applicability of the modeled results in seismic risk assessment, an empirical seismic loss estimation is performed based on the intensity map of the 2008 Wenchuan Ms8.0 earthquake, the empirical loss function in Daniell (2014), and our modelled replacement value of residential buildings in Sichuan province. By reducing the difference in unit construction price used in this paper and other studies, our estimated loss range is consistent with the loss derived from damage reports based on field investigation. These comparisons indicate the reliability of the geo-coded grid level residential building exposure model developed in this paper. More importantly, the whole modeling process is fully reproducible, and

all the modeled results are available from the online supplement, which can also be easily updated when more recent or detailed census data are available.

Appendix

In Appendix A, to derive the population living in each of the 17 building subtypes of each grid, the distribution
645　strategy mentioned in Sect. 2.4.2 is explained in detail. In addition, a MATLAB script is provided to help understand this strategy.

Data/Code Availability

The accesses to data used or mentioned in this paper are as follows: (1) 2010 China Sixth Population Census Tab ulation (http://www.stats.gov.cn/tjsj/pcsj/rkpc/6rp/indexch.htm); (2) 2015 Global Human Settlement Layer (GHS
650　L) population density profile (http://data.europa.eu/89h/jrc-GHS-ghs_pop_gpw4_globe_r2015a) ; (3) The spatial administrative boundaries from the National Geomatics Centre of China (http://www.ngcc.cn/ngcc/html/1/391/3 92/16114.html); (4) The Globcover land cover maps (http://due.esrin.esa.int/page_globcover.php); (5) The GLC2 000 landcover classes (https://forobs.jrc.ec.europa.eu/products/glc2000/legend.php); (6) The MODIS imaging pr oject (https://modis.gsfc.nasa.gov/about/); (7) The GlobeLand30 project (http://www.globallandcover.com/); (8)
655　The DMSP-OLS nighttime light datasets (https://data.noaa.gov/metaview/page?xml=NOAA/NESDIS/NGDC/ST P/DMSP/iso/xml/G01119.xml&view=getDataView&header=none); (9) OpenStreetMap (https://www.openstreet map.org/); (10) Gridded Population of the World (GPW, http://sedac.ciesin.columbia.edu/gpw/global.jsp); (11) G lobal Rural-Urban Mapping Project-Population (GRUMP-population, https://sedac.ciesin.columbia.edu/data/coll ection/grump-v1); (12) LandScan Global Population Datasets (https://landscan.ornl.gov/landscan-datasets); (13)
660　WorldPop/AsianPop (https://www.worldpop.org/geodata/listing?id=29); (14) PopGrid China (http://www.geodo i.ac.cn/edoi.aspx?DOI=10.3974/geodb.2014.01.06.V1); (15) An example illustrating the multi-variate equation s olving process in Sect. 2.4.2, including the input file and the MATLAB script that are available from the online s upplement.

Supplement

665　The supplementary data related to this work are available online at https://doi.org/10.5281/zenodo.4669800.

Author contribution

DX conducted the data collection and preparation, analyses of results, model validation, and prepared the draft manuscript. JD guided the data collection and preparation process, developed the modeling methodology and performed the calculation and co-analysed the results. HT and FW supervised the project and provided advice and
670　feedback in the process. All authors contributed to the revision of the manuscript.

Competing interests

The authors declare that they have no conflict of interests.

18

Acknowledgements

References

Allen, T. I., Wald, D. J., Earle, P. S., Marano, K. D., Hotovec, A. J., Lin, K. and Hearne, M. G.: An Atlas of ShakeMaps and population exposure catalog for earthquake loss modeling, Bull Earthquake Eng, 7(3), 701–718, doi:10.1007/s10518-009-9120-y, 2009.

Aubrecht, C. and León Torres, J. A.: Top-down identification of mixed vs. residential use in urban areas: Evaluation of remotely sensed nighttime lights for a case study in Cuenca City, Ecuador, in: Proceedings of the 1st International Electronic Conference on Remote Sensing, 22 June-5 July 2015, online (sciforum.net), available at: https://www.researchgate.net/publication/300483105 (last access: 17 January 2021), 2015.

Aubrecht, C., Steinnocher, K., K O Stl, M., Z U Ger, J. and Loibl, W.: Long-term spatio-temporal social vulnerability variation considering health-related climate change parameters particularly affecting elderly, Natural Hazards, 68(3), 1371–1384, doi:10.1007/s11069-012-0324-0, 2013.

Bal, I. E., Bommer, J. J., Stafford, P. J., Crowley, H., and Pinho, R.: The Influence of Geographical Resolution of Urban Exposure Data in an Earthquake Loss Model for Istanbul, Earthquake Spectra, 26, 619–634, doi:10.1193/1.3459127, 2010.

Balk, D. and Yetman, G.: The global distribution of population: evaluating the gains in resolution refinement, Center for International Earth Science Information Network (CIESIN), Columbia University, New York, USA, available at https://www.researchgate.net/publication/228735948 (last access: 17 January 2021), 2004.

Bhaduri, B., Bright, E., Coleman, P. and Urban, M. L.: LandScan USA: a high-resolution geospatial and temporal modeling approach for population distribution and dynamics, GeoJournal, 69(1–2), 103–117, doi:10.1007/s10708-007-9105-9, 2007.

Bing Maps Team: Over 100 New Streetside and 3D Cities Go Live on Bing Maps, available at https://blogs.bing.com/maps/2014/08/20/over-100-new-streetside-and-3d-cities-go-live-on-bing-maps/ (last access: 17 January 2021), 2014.

Bird, J. F. and Bommer, J. J.: Earthquake losses due to ground failure, Engineering Geology, 75(2), 147–179, doi: 10.1016/j.enggeo.2004.05.006, 2004.

Cao, Y. and Huang, X.: A deep learning method for building height estimation using high-resolution multi-view imagery over urban areas: A case study of 42 Chinese cities, Remote Sensing of Environment, 264(2021), 112590, do:10.1016/j.rse.2021.112590, 2021.

Chen, K., McAneney, J., Blong, R., Leigh, R., Hunter, L. and Magill, C.: Defining area at risk and its effect in catastrophe loss estimation: a dasymetric mapping approach, Applied Geography, 24(2), 97–117, doi: 10.1016/j.apgeog.2004.03.005, 2004.

Chen, X. and Nordhaus, W. D.: Using luminosity data as a proxy for economic statistics, Proceedings of the National Academy of Sciences, 108(21), 8589–8594, doi:10.1073/pnas.1017031108, 2011.

Chen, Z., Li, Z., Ding, W. and Han, Z.: Study of Spatial Population Distribution in Earthquake Disaster Reduction ---- A Case Study of 2007 Ning'er Earthquake, Technology for Earthquake Disaster Prevention, 7(3), 273–284, doi:10.3969/j.issn.1673-5722.2012.03.006, 2012 (in Chinese).

Corbane, C., Hancilar, U., Ehrlich, D. and De Groeve, T.: Pan-European seismic risk assessment: a proof of concept using the Earthquake Loss Estimation Routine (ELER), Bulletin of Earthquake Engineering, 15(3), 1057–1083, doi: 10.1007/s10518-016-9993-5, 2017.

Dabbeek, J., Crowley, H., Silva, V., Weatherill, G., Paul, N., and Nievas, C. I.: Impact of exposure spatial resolution on seismic loss estimates in regional portfolios, Bulletin of Earthquake Engineering, doi:10.1007/s10518-021-01194-x, 2021.

Daniell, J.: Development of socio-economic fragility functions for use in worldwide rapid earthquake loss estimation procedures, Ph.D. Thesis, Karlsruhe Institute of Technology, Karlsruhe, Germany, 2014.

Daniell, J. E., Schaefer, A. M. and Wenzel, F.: Losses Associated with Secondary Effects in Earthquakes, Front. Built Environ., 3, doi:10.3389/fbuil.2017.00030, 2017.

De Bono, A. and Chatenoux, B.: A global exposure model for GAR 2015, United Nations International Strategy for Disaster Reduction, Geneva, Switzerland, available at https://www.researchgate.net/publication/275639260 (last access: 17 January 2021), 2015.

De Bono, A. and Mora, M. G.: A global exposure model for disaster risk assessment, International Journal of Disaster Risk Reduction, 10(2014), 442–451, doi:10.1016/j.ijdrr.2014.05.008, 2014.

De Bono, A., Chatenoux, B., Herold, C. and Peduzzi, P.: Global Assessment Report on Disaster Risk Reduction 2013: From shared risk to shared value-The business case for disaster risk reduction, United Nations International Strategy for Disaster Reduction, Geneva, Switzerland, available at https://archive-ouverte.unige.ch/unige:32532 (last access: 17 January 2021), 2013.

20

Dell'Acqua, F., Gamba, P. and Jaiswal, K.: Spatial aspects of building and population exposure data and their implications for global earthquake exposure modeling, Natural Hazards, 68(3), 1291–1309, doi:10.1007/s11069-012-0241-2, 2013.

740 Dobson, J. E., Bright, E. A., Coleman, P. R., Durfee, R. C. and Worley, B. A.: LandScan: a global population database for estimating populations at risk, Photogrammetric Engineering and Remote Sensing, 66(7), 849–857, available at https://www.researchgate.net/publication/267450852 (last access: 17 January 2021), 2000.

Doll, C. N. H., Muller, J.-P. and Morley, J. G.: Mapping regional economic activity from night-time light satellite imagery, Ecological Economics, 57(1), 75–92, doi:10.1016/j.ecolecon.2005.03.007, 2006.

Eicher, C. L. and Brewer, C. A.: Dasymetric Mapping and Areal Interpolation: Implementation and Evaluation, 745 Cartography and Geographic Information Science, 28(2), 125–138, doi:10.1559/152304001782173727, 2001.

Elvidge, C. D., Tuttle, B. T., Sutton, P. C., Baugh, K. E., Howard, A. T., Milesi, C., Bhaduri, B. and Nemani, R.: Global distribution and density of constructed impervious surfaces, Sensors, 7(9), 1962–1979, available at https://www.mdpi.com/1424-8220/7/9/1962/pdf (last access: 17 January 2021), 2007.

EPERDR: Expert Panel of Earthquake Resistance and Disaster Relief: Comprehensive Disaster and Risk Analysis 750 of Wenchuan Earthquake, Science Press, Beijing, China, 2008 (in Chinese).

Erdik, M.: Earthquake risk assessment, Bulletin of Earthquake Engineering, 15(12), 5055–5092, https://doi.org/10.1007/s10518-017-0235-2, 2017.

Figueiredo, R. and Martina, M.: Using open building data in the development of exposure data sets for catastrophe risk modeling, Natural Hazards and Earth System Sciences, 16(2), 417–429, doi:10.5194/nhess-16-417-2016, 755 2016.

Freire, S., MacManus, K., Pesaresi, M., Doxsey-Whitfield, E. and Mills, J.: Development of new open and free multi-temporal global population grids at 250m resolution, in: Proceedings of the 19th AGILE Conference on Geographic Information Science, 14-17 June 2016, Helsinki, Finland, available at https://www.researchgate.net/publication/304625387 (last access: 17 January 2021), 2016.

760 Fu, J., Jiang, D. and Huang, Y.: Populationgrid_China, Acta Geographica Sinica, 69(Supplement), 41–44, doi: 10.11821/dlxb2014S006, 2014a (in Chinese).

Fu, J., Jiang, D. and Huang, Y.: 1 KM Grid Population Dataset of China, doi:10.3974/geodb.2014.01.06.V1, 2014b (in Chinese).

Fuchs, S., Keiler, M., and Zischg, A.: A spatiotemporal multi-hazard exposure assessment based on property data, 765 Nat. Hazards Earth Syst. Sci., 15, 2127–2142, doi:10.5194/nhess-15-2127-2015, 2015.

Gamba, P.: Global Exposure Database: Scientific Features, Global Earthquake Model (GEM) Foundation, Pavia, Italy, available at https://storage.globalquakemodel.org/resources/publications/technical-reports/global-exposure-database-scientific-features/ (last access: 17 January 2021), 2014.

Gaughan, A. E., Stevens, F. R., Linard, C., Jia, P. and Tatem, A. J.: High Resolution Population Distribution Maps for Southeast Asia in 2010 and 2015, PLoS ONE, 8(2), e55882, doi:10.1371/journal.pone.0055882, 2013.

Ghosh, T., L Powell, R., D Elvidge, C., E Baugh, K., C Sutton, P. and Anderson, S.: Shedding light on the global distribution of economic activity, The Open Geography Journal, 3(1), available at https://www.researchgate.net/publication/228371381 (last access: 17 January 2021), 2010.

Goodchild, M. F., Anselin, L. and Deichmann, U.: A Framework for the Areal Interpolation of Socioeconomic Data, Environ Plan A, 25(3), 383–397, doi:10.1068/a250383, 1993.

Gunasekera, R., Ishizawa, O., Aubrecht, C., Blankespoor, B., Murray, S., Pomonis, A. and Daniell, J.: Developing an adaptive global exposure model to support the generation of country disaster risk profiles, Earth-Science Reviews, 150, 594–608, doi:10.1016/j.earscirev.2015.08.012, 2015.

Han, Z., Li, Z., Chen, Z., Ding, W. and Wang, L.: Population, Housing Statistics Data Spatialization Research in the Application of Rapid Earthquake Loss Assessment ---- A Case of Yiliang Earthquake, Seismology and Geology, 35(4), 894–906, doi:10.3969/j.issn.0253-4967.2013.04.018, 2013 (in Chinese).

Holz, C. A.: New capital estimates for China, China Economic Review, 17(2), 142–185, doi: 10.1016/j.chieco.2006.02.004, 2006.

Hu, D., Zhang, F., Xiao, X., Shi, Q., Li, L., Zhang, Z. and Wang, X.: Survey and Statistical Study of Rural Buildings in Southwest China, Earthquake Resistant Engineering and Retrofitting, 37(3), 113–120, doi: 10.16226/j.issn.1002-8412.2015.03.019, 2015 (in Chinese).

Hu, M., Bergsdal, H., Voet, E. van der, Huppes, G. and Müller, D. B.: Dynamics of urban and rural housing stocks in China, Building Research & Information, 38(3), 301–317, doi:10.1080/09613211003729988, 2010.

Jaiswal, K., Wald, D. and Porter, K.: A global building inventory for earthquake loss estimation and risk management, Earthquake Spectra, 26(3), 731–748, doi:10.1193/1.3450316, 2010.

Ji, H., Li, X., Wei, X., Liu, W., Zhang, L. and Wang, L.: Mapping 10-m Resolution Rural Settlements Using Multi-Source Remote Sensing Datasets with the Google Earth Engine Platform, Remote Sensing, 12(17), 2832, doi:10.3390/rs12172832, 2020.

Jiang, D., Yang, X., Wang, N. and Liu, H.: Study on spatial distribution of population based on remote sensing and GIS, Advances in Earth Sciences, 17(5), 734–738, doi:10.3321/j.issn:1001-8166.2002.05.016, 2002 (in Chinese).

Li, M., Koks, E., Taubenböck, H., and van Vliet, J.: Continental-scale mapping and analysis of 3D building structure, Remote Sensing of Environment, 245(2020), 111859, doi:/10.1016/j.rse.2020.111859, 2020.

Lin, D., Tan, M., Liu, K., Liu, L. and Zhu, Y.: Accuracy Comparison of Four Gridded Population Datasets in Guangdong Province, China, Tropical Geography, 40(2), 346–356, doi:10.13284/j.cnki.rddl.003220, 2020 (in Chinese).

Linard, C., Gilbert, M., Snow, R. W., Noor, A. M. and Tatem, A. J.: Population distribution, settlement patterns and accessibility across Africa in 2010, PloS one, 7(2), e31743, doi:10.1371/journal.pone.0031743, 2012.

Liu, M., Ma, J., Zhou, R., Li, C., Li, D., and Hu, Y.: High-resolution mapping of mainland China's urban floor area, Landscape and Urban Planning, 214(2021), 104187, doi:10.1016/j.landurbplan.2021.104187, 2021.

Lu, L., Guo, H., Pesaresi, M., Soille, P. and Ferri, S.: Automatic Recognition of Built-up Areas in China Using CBERS-2B HR Data, in: Proceedings of the JURSE 2013, 21-23 April 2013, São Paulo, Brazil, available at https://publications.jrc.ec.europa.eu/repository/handle/JRC86187 (last access: 17 January 2021), 2013.

Ma, T., Zhou, C., Pei, T., Haynie, S. and Fan, J.: Quantitative estimation of urbanization dynamics using time series of DMSP/OLS nighttime light data: A comparative case study from China's cities, Remote Sensing of Environment, 124, 99–107, doi:10.1016/j.rse.2012.04.018, 2012.

Messner, F. and Meyer, V.: FLOOD DAMAGE, VULNERABILITY AND RISK PERCEPTION – CHALLENGES FOR FLOOD DAMAGE RESEARCH, in: Flood Risk Management: Hazards, Vulnerability and Mitigation Measures, edited by: Schanze J., Zeman E., and Marsalek J., Springer, Dordrecht, Netherlands, 149–167, doi: 10.1007/978-1-4020-4598-1_13, 2006.

Neumayer, E. and Barthel, F.: Normalizing economic loss from natural disasters: a global analysis, Global Environmental Change, 21(1), 13–24, doi:10.1016/j.gloenvcha.2010.10.004, 2011.

Paprotny, D., Kreibich, H., Morales-Nápoles, O., Terefenko, P. and Schröter, K.: Estimating exposure of residential assets to natural hazards in Europe using open data, Natural Hazards and Earth System Sciences, 20(1), 323–343, doi:10.5194/nhess-20-323-2020, 2020.

Parikh, B.: Expanded coverage of building footprints in Google Maps, available at http://google-latlong.blogspot.com/2012/10/expanded-coverage-of-building.html (last access: 17 January 2021), 2012.

Pesaresi, M., Huadong, G., Blaes, X., Ehrlich, D., Ferri, S., Gueguen, L., Halkia, M., Kauffmann, M., Kemper, T., Lu, L., Marin-Herrera, M. A., Ouzounis, G. K., Scavazzon, M., Soille, P., Syrris, V. and Zanchetta, L.: A Global Human Settlement Layer From Optical HR/VHR RS Data: Concept and First Results, IEEE J. Sel. Top. Appl. Earth Observations Remote Sensing, 6(5), 2102–2131, doi:10.1109/JSTARS.2013.2271445, 2013.

Pesaresi, M., Ehrlich, D., Ferri, S., Florczyk, A. J., Freire, S., Halkia, M., Julea, A., Kemper, T., Soille, P. and Syrris, V.: Operating procedure for the production of the Global Human Settlement Layer from Landsat data of the epochs 1975, 1990, 2000, and 2014, Jlint Research Center (JRC) Technical Reports, European Commission, Ispra (VA), Italy, doi:10.2788/253582, 2016.

Röthlisberger, V., Zischg, A. P., and Keiler, M.: A comparison of building value models for flood risk analysis, Nat. Hazards Earth Syst. Sci., 18, 2431–2453, doi:10.5194/nhess-18-2431-2018, 2018.

Sabesan, A., Abercrombie, K., Ganguly, A. R., Bhaduri, B., Bright, E. A. and Coleman, P. R.: Metrics for the comparative analysis of geospatial datasets with applications to high-resolution grid-based population data, GeoJournal, 69(1), 81–91, doi:10.1007/s10708-007-9103-y, 2007.

Seifert, I., Thieken, A. H., Merz, M., Borst, D. and Werner, U.: Estimation of industrial and commercial asset values for hazard risk assessment, Natural Hazards, 52(2), 453–479, doi:10.1007/s11069-009-9389-9, 2010.

Silva, V., Crowley, H., Varum, H. and Pinho, R.: Seismic risk assessment for mainland Portugal, Bulletin of Earthquake Engineering, 13(2), 429–457, doi:10.1007/s10518-014-9630-0, 2015.

840 Thieken, A. H., M U Ller, M., Kleist, L., Seifert, I., Borst, D. and Werner, U.: Regionalisation of asset values for risk analyses, Natural Hazards and Earth System Sciences, 6(2), 167–178, doi:10.5194/nhess-6-167-2006, 2006.

Tobler, W.: Smooth Pycnophylactic Interpolation for Geographic Regions, Journal of American Statistical Association, 74(367), 519–530, doi:10.1080/01621459.1979.10481647, 1979.

Wang, L. and Szirmai, A.: Capital inputs in the Chinese economy: Estimates for the total economy, industry and 845 manufacturing, China Economic Review, 23(1), 81–104, doi:10.1016/j.chieco.2011.08.002, 2012.

Wang, Z., Yi, W. and Wang, M.: Statistical analysis of natural vibration period of high-rise and super high-rise concrete and steel-reinforced concrete mixed structures in China, Building Structure, 48(3), 85–89, doi:10.19701/j.jzjg.2018.03.016, 2018 (in Chinese).

Wu, J., Li, N. and SHI, P.: Benchmark wealth capital stock estimations across China's 344 prefectures: 1978 to 850 2012, China Economic Review, 31, 288–302, doi:10.1016/j.chieco.2014.10.008, 2014.

Wu, J., Li, Y., Li, N. and Shi, P.: Development of an asset value map for disaster risk assessment in China by spatial disaggregation using ancillary remote sensing data, Risk Analysis, 38(1), 17–30, doi:10.1111/risa.12806, 2018.

Wu, J., Ye, M., Wang, X. and Koks, E.: Building asset value mapping in support of flood risk assessments: A case 855 study of Shanghai, China, Sustainability, 11(4), 971, doi:10.3390/su11040971 2019.

Wu, Z., Ma, T., Jiang, H. and Jiang, C.: Multi-scale seismic hazard and risk in the China mainland with implication for the preparedness, mitigation, and management of earthquake disasters: An overview, International Journal of Disaster Risk Reduction, 4, 21–33, doi:10.1016/j.ijdrr.2013.03.002, 2013.

Wünsch, A., Herrmann, U., Kreibich, H. and Thieken, A. H.: The Role of Disaggregation of Asset Values in Flood 860 Loss Estimation: A Comparison of Different Modeling Approaches at the Mulde River, Germany, Environmental Management, 44(3), 524–541, doi:10.1007/s00267-009-9335-3, 2009.

Xiong, C.: Automated regional seismic damage assessment of buildings using an unmanned aerial vehicle and a convolutional neural network, Automation in Construction, 14, doi:10.1016/j.autcon.2019.102994, 2020.

Xu, J., An, J. and Nie, G.: A quick earthquake disaster loss assessment method supported by dasymetric data for 865 emergency response in China, Natural Hazards and Earth System Sciences, 16, 885–899, doi:10.5194/nhess-16-885-2016, 2016a.

24

Xu, J., An, J. and Nie, G.: Development of Earthquake Emergency Disaster Information Pre-Evaluation Data Based on km Grid, Seismology and Geology, 38(3), 760–772, doi:10.3969/j.issn.0253-4967.2016.03.020, 2016b (in Chinese).

870   Yang, W. and Kohler, N.: Simulation of the evolution of the Chinese building and infrastructure stock, Building Research and Information, 36(1), 1–19, doi:10.1080/09613210701702883, 2008.

Yuan, Y.: Impact of intensity and loss assessment following the great Wenchuan Earthquake, Earthquake Engineering and Engineering Vibration, 7(3), 247–254, doi: 10.1007/s11803-008-0893-9, 2008.

Zhang, Y., Li, X., Wang, A., Bao, T. and Tian, S.: Density and diversity of OpenStreetMap road networks in 875   China, Journal of Urban Management, 4(2), 135–146, doi:10.1016/j.jum.2015.10.001, 2015.
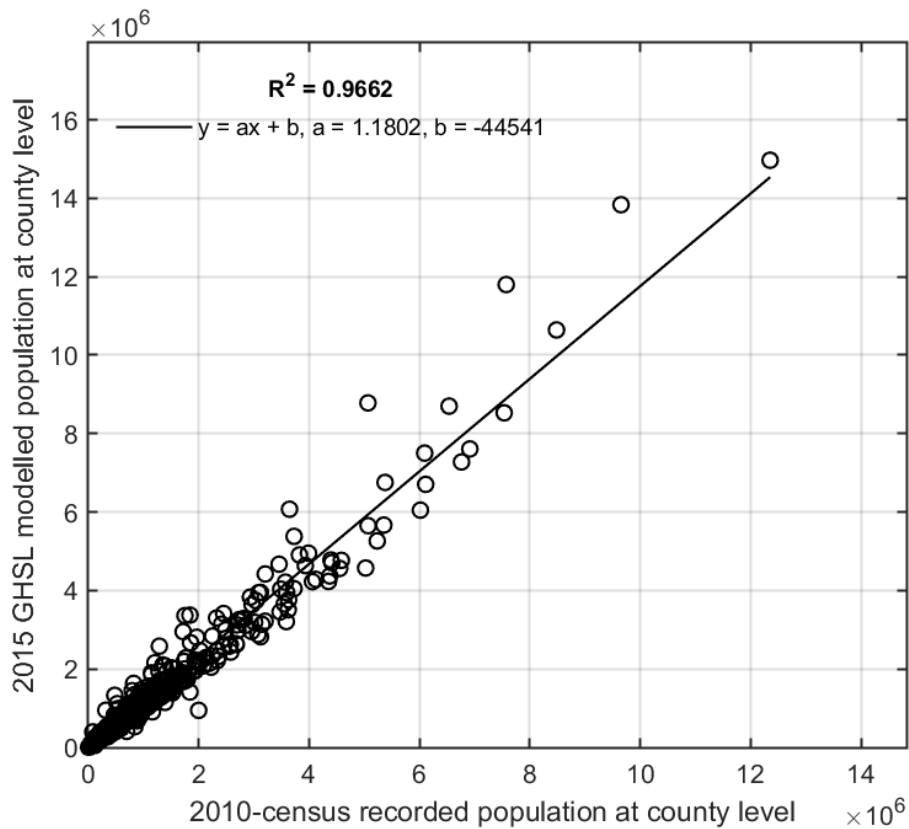
Figure 1: County-level comparison of the population between the 2015 GHSL profile and the 2010-census records.
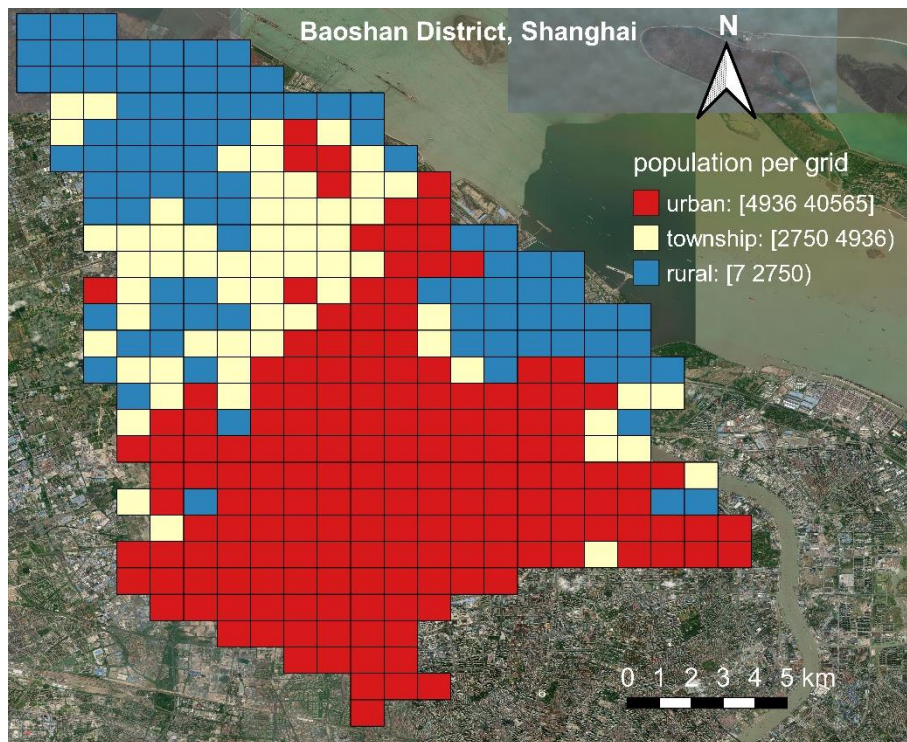
880

Figure 2: An example showing the assignment of urbanity attribute in the 2015 GHSL population grids for Baoshan district in Shanghai. The urban/township and township/rural population thresholds for Shanghai are 4936/km^2 and 2750/km^2, respectively (see context in **Sect. 2.3** for more details). This figure is plotted by using the

QGIS platform (https://qgis.org/en/site/) and the background satellite map is provided by Bing map service (© Microsoft).
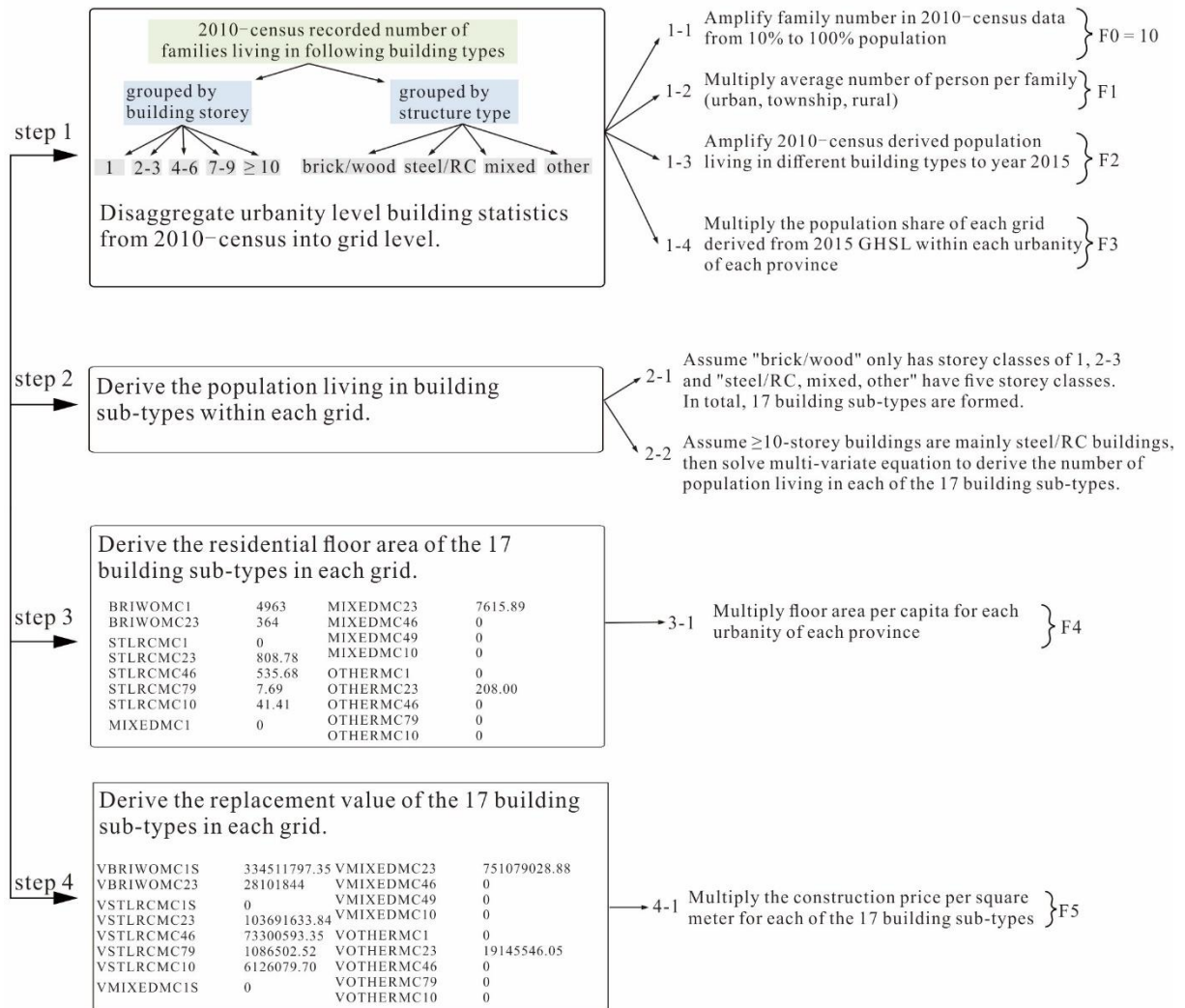
Modeling Process

Figure 3: Flowchart of the residential building stock modeling process adopted in this paper (see context in **Sect. 2.4** for more details).
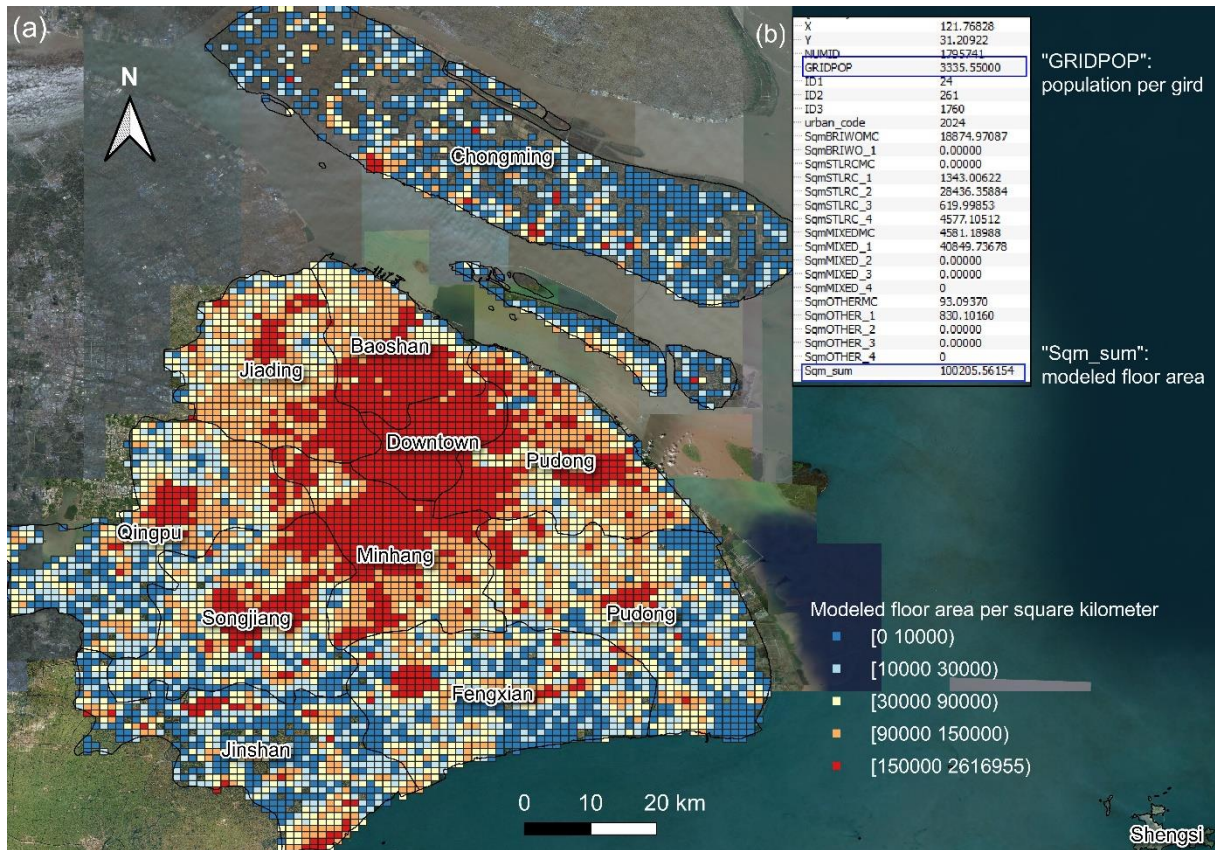
890

e

Figure 4. An example illustrating the building stock model of Shanghai: (a) The distribution of modeled floor area (unit: m^2) in each 1km×1km grid (note that the legend in Figure 4 is different from that in Figure 2); (b) A table showing the modeled floor area of the 17 building subtypes, the total population "GRIDPOP" and the total modeled floor area "Sqm_sum" in an example grid. This figure is plotted by using the QGIS platform and the background
895   satellite map is provided by the Bing map service (© Microsoft).

28
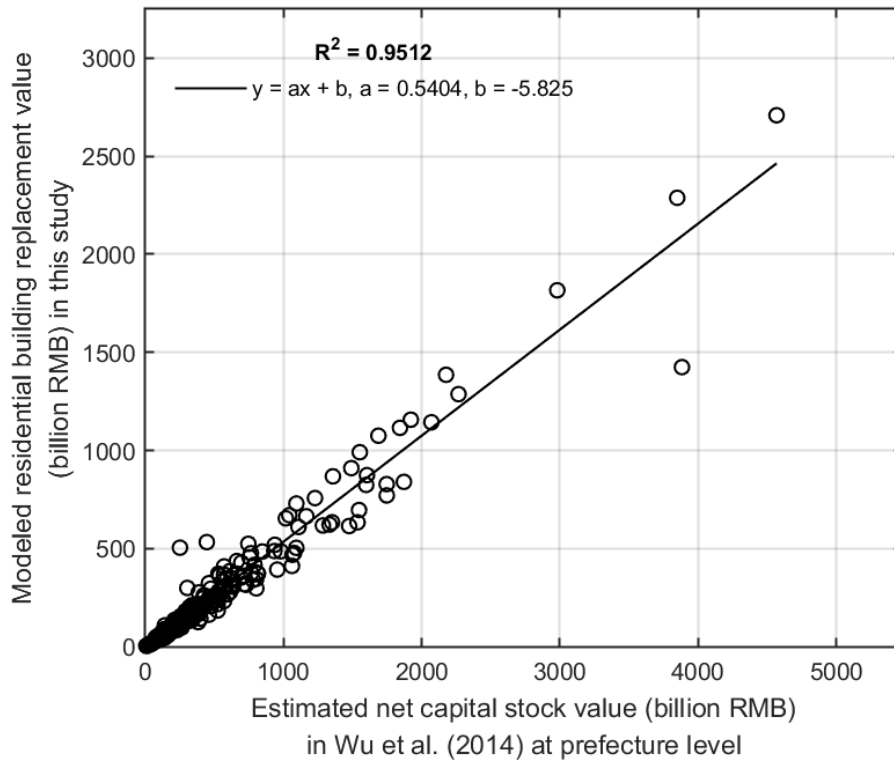
Figure 5: Prefecture-level comparison of the modeled residential building replacement value in this paper (unit: billion RMB in 2015 current price) with the net capital stock value estimated in Wu et al. (2014) by using the perpetual inventory method (unit: billion RMB in 2012 current price). Note: the net capital stock value estimated in Wu et al. (2014) includes the depreciated value of all exposed elements, namely the residential buildings, non-residential buildings, infrastructures, and equipment (see context in **Sect. 3.2.1** for more details).

900
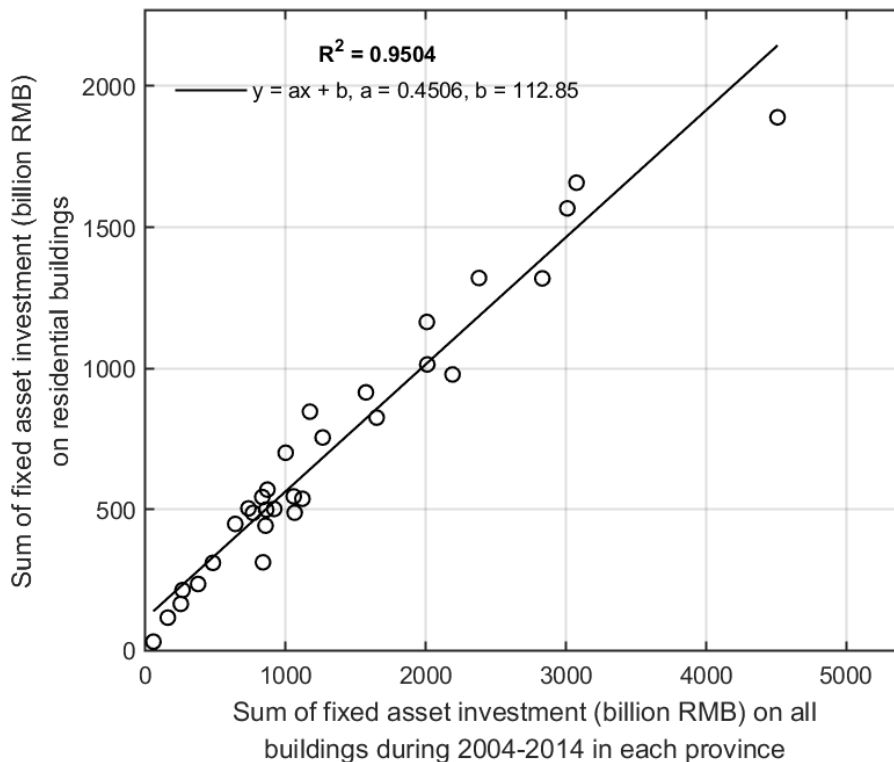
Figure 6: Comparison of the sum of the annual fixed asset investment (unit: billion RMB) on residential buildings with investment on all types of buildings during 2004-2014 in each of the 31 provinces in mainland China. Detailed investment statistics are available from the online supplement.
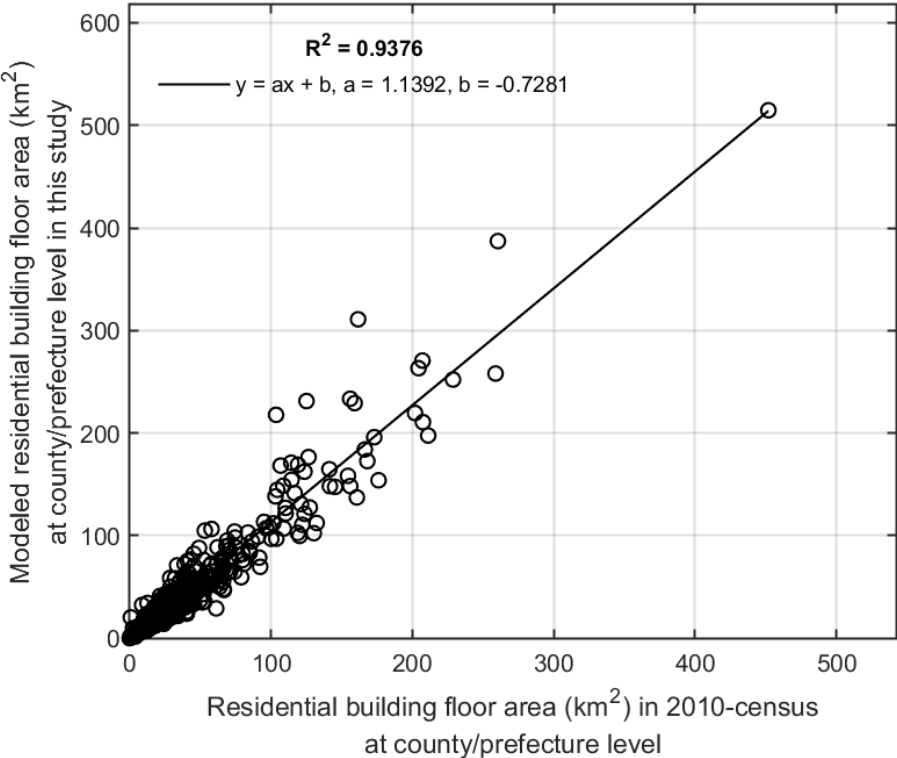
Figure 7: County/prefecture-level comparison of the modeled residential building floor area (km^2) in this paper with that recorded in the 2010-census for 31 provinces in mainland China (see context in **Sect. 3.2.2** for more details).

Intensity map of 2008.05.12 Wenchuan Ms8.0 earthquake
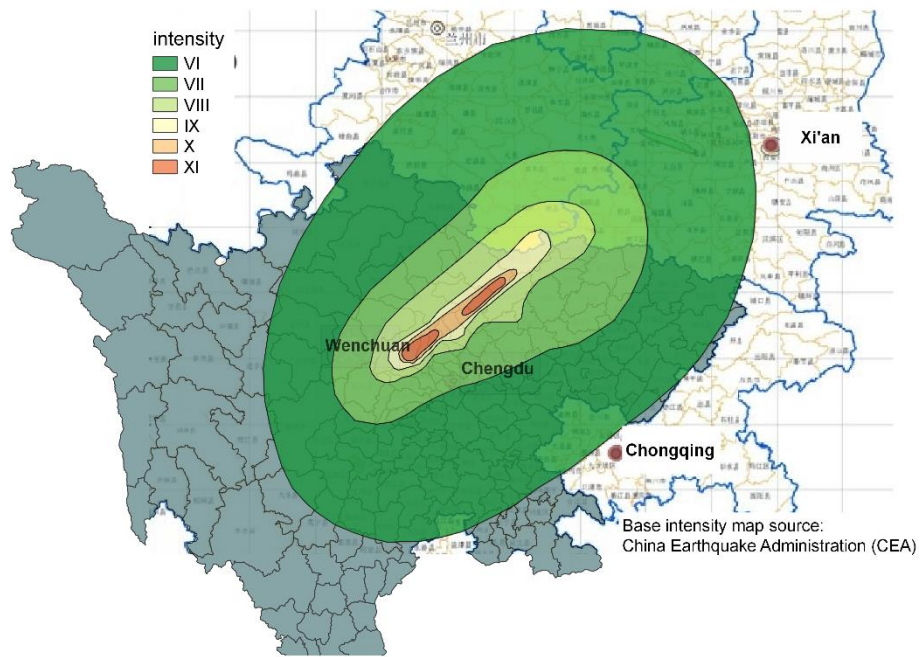
Figure 8. Macro-seismic intensity map of the 2008 Wenchuan Ms8.0 earthquake, modified after the base intensity map issued by China Earthquake Administration (CEA).
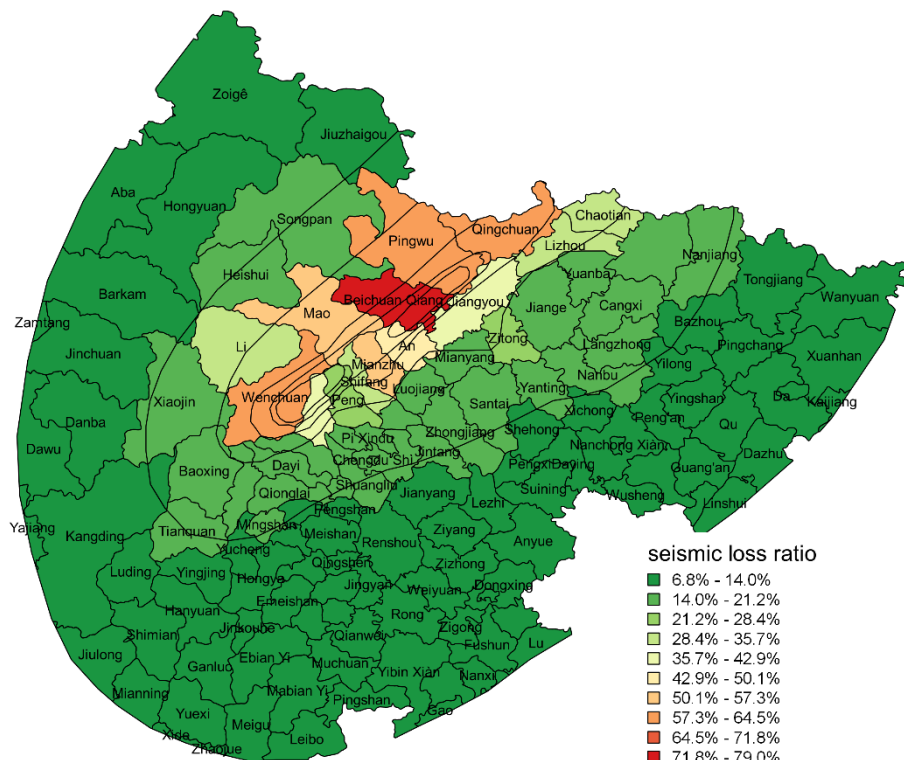
915

Figure 9. Distribution of seismic loss ratio (the ratio between repairment cost and replacement cost) of residential buildings in affected districts/counties of Sichuan province due to the 2008 Wenchuan Ms8.0 earthquake. Black contours represent the extent of each intensity zone of the Wenchuan earthquake (see context in **Sect. 3.2.3** for more details).

Tables

Table 1: Main data sources used in this paper. Accesses to these data are provided in the Data/Code Availability section.

Data source	Data description	Resolution	Data location	Indicator in this paper	Notes
2010-census Short Table	Overall population	urban/township/rural level for each of the 31 provinces in mainland China; (the urbanity level in the census is defined according to the administrative unit of the surveyed population)	Table 1-1a, 1-1b, 1-1c	N/A	Based on surveys of 100% of the population in mainland China
2010 -census Long Table	Number of families living in buildings grouped by usage (residential, commercial, mixed)		Table 9-1a, 9-1b, 9-1c	N/A	Based on surveys of 10% of the overall population in mainland China
	Number of families dwelled in buildings grouped by storey number (1, 2-3, 4-6, 7-9, ≥10)				
	Number of families dwelled in buildings grouped by structuretype (steel/RC, mixed, other, brick/wood)				
2010-census Short Table	Average population per family		Table 1-1a, 1-1b, 1-1c	F2 of Fig. 3	Based on surveys of 100% of the population in mainland China
	Average residential floor area (m^2) per person		Table 1-14a, 1-14b, 1-14c	F4 of Fig. 3	
2015 GHSL population density profile	The number of populations in each geo-coded grid	1km×1km	N/A	λ	The original resolution is 250m×250m and was resampled to 1km×1km
Wu et al. (2014)	The estimated net wealth capital stock value in 344 prefectures of mainland China	Prefecture-level	N/A	N/A	All exposed assets (residential and non-residential buildings, infrastructures, instruments, etc.) and their depreciation are considered
2010-census Short Table	The residential building floor area statistics in administrative units	Prefecture-level for Hunan, Liaoning, and Sichuan; county-level for other 28 provinces	Table 1-1, 1-14 in the 2010-census book of each province	N/A	Some data are downloaded from the commercial website (https://www.yearbookchina.com/)

Note: The "2010-census" in "**Data source**" is the abbreviation of the "2010 Population Census of the People's Republic of China"; "**Data location**" refers to the serial number of the table in the original data source (see context in **Sect. 2.1** for more details).

925

Table 2: In each urbanity, the population sum of the 2015 GHSL profile and the residential building-related statistics extracted from the 2010-census records.

"Urbanity"+"0"+"Prov_ID"	Province	2015 GHSL population in each urbanity	Floor area per capita (m²)	Aver. pop. per family	Number of families grouped by occupancy			Number of families grouped by storey class					Number of families grouped by structure type				Amp. factor
					living	commercial	mixed	1	2-3	4-6	7-9	≥10	steel/RC	mixed masonry	brick/wood	other	
urban																	
1001	Anhui	12165295	29.42	2.71	331730	9035	287	44093	82489	175486	20922	17775	135377	176462	26705	2221	1.32
1002	Beijing	18598941	27.81	2.40	517975	6482	988	127740	33290	193270	21919	148238	226367	212873	83192	2025	1.47
1003	Chongqing	8402588	29.77	2.65	258417	3956	247	17185	39448	39087	85383	81270	131656	112494	13433	4790	1.21
1004	Fujian	12702780	30.29	2.70	360721	13488	736	30557	97680	135725	79915	30332	213350	124702	23948	12209	1.25
1005	Gansu	5296224	26.69	2.68	160717	3134	107	24489	21076	75051	34161	9074	78731	66665	15057	3398	1.21
1006	Guangdong	56529958	26.37	2.63	1466895	34218	513	152601	299326	453172	412315	183699	748196	663772	76682	12463	1.43
1007	Guangxi	8484803	30.71	2.93	238044	5912	264	26305	53876	99335	52485	11955	86601	138730	16271	2354	1.19
1008	Guizhou	5475276	25.94	2.82	157713	5141	19	17373	38055	50766	49256	7404	78055	75834	7703	1262	1.19
1009	Hainan	2334559	25.42	3.17	56383	1602	68	9674	14288	13787	13124	7112	41510	10814	4948	713	1.27
1010	Hebei	14837665	30.10	2.95	419978	3950	96	100741	42944	230919	29889	19435	155581	211716	54745	1886	1.19
1011	Heilongjiang	14368585	23.72	2.58	455996	6911	418	122051	20020	130862	173283	16691	163427	188650	104208	6622	1.20
1012	Henan	18535815	34.02	3.05	521036	7612	215	79535	122569	244091	64920	17533	190648	307902	28268	1830	1.15
1013	Hubei	17545544	33.22	2.82	502439	12733	349	40937	132838	179474	126270	35653	180316	298109	33900	2847	1.21
1014	Hunan	12920714	33.45	2.89	358447	9813	501	32935	92165	160007	62887	20266	132713	201615	31404	2528	1.21
1015	Jiangsu	30871919	33.86	2.81	876264	14961	802	129293	224580	412115	65052	60185	325288	469388	92721	3828	1.23
1016	Jiangxi	7845049	29.76	3.19	201690	3594	201	17052	46727	85663	48457	7385	111658	76679	15396	1551	1.20
1017	Jilin	10272119	25.21	2.62	329782	4910	1777	59861	13029	149906	96067	15829	175788	108325	48852	1727	1.17
1018	Liaoning	22179450	25.76	2.57	768884	7122	843	111439	28046	366106	211530	58885	321935	381031	71386	1654	1.11
1019	Inner Mongolia	8313523	24.86	2.67	251738	6951	631	84432	24977	133932	11690	3658	105902	87092	61924	3771	1.20
1020	Ningxia	2222156	28.38	2.71	64336	1829	29	10922	7958	44770	1313	1202	24606	34483	6352	724	1.24
1021	Qinghai	1478166	27.77	2.74	41342	1229	62	4877	8035	20737	6292	2630	13527	26113	2415	516	1.27
1022	Shaanxi	9028318	28.81	2.70	269044	4820	362	33723	56478	122687	37356	23620	89287	173753	8694	2130	1.22
1023	Shandong	28926001	32.41	2.80	855282	15616	242	252471	88326	432226	67205	30670	348873	356038	161295	4692	1.19
1024	Shanghai	20564236	25.11	2.52	604654	9991	928	60506	116799	304794	27780	104766	268377	249438	93734	3096	1.33
1025	Shanxi	9838476	25.77	2.88	282847	4319	87	53815	47879	157087	18683	9702	90187	163209	29124	4646	1.19
1026	Sichuan	15739421	30.70	2.67	499024	9628	630	47158	79975	198299	136824	46396	218827	247875	34088	7862	1.16
1027	Tianjin	10012784	25.51	2.65	237060	2606	167	34902	12083	143755	28570	20356	58333	156521	23467	1345	1.58
1028	Xinjiang	6579942	28.00	2.56	201621	2686	84	32261	24343	129144	12124	6435	88699	94628	18420	2560	1.26
1029	Tibet	286242	31.81	2.45	8394	973	7	2930	4798	1580	47	12	5449	2227	1020	671	1.25
1030	Yunnan	6548268	31.27	2.59	200602	7122	172	21262	45555	93027	36704	11176	102015	85386	13317	7006	1.22
1031	Zhejiang	21735537	30.97	2.54	675858	19305	774	80859	193447	332899	50666	37292	220048	393843	74559	6713	1.23
township																	
2001	Anhui	13378847	32.20	2.95	355306	19130	477	144219	160370	67744	1426	677	95625	182264	91921	4626	1.21
2002	Beijing	1548170	33.20	2.52	41959	1129	143	21808	2812	16414	710	1344	6224	20550	15964	350	1.42
2003	Chongqing	6401393	34.91	2.73	187287	7816	357	35957	71385	40448	41156	6157	46425	112018	23805	12855	1.20
2004	Fujian	8618108	37.67	3.09	224647	11851	318	44154	105240	65529	18822	2753	100650	83984	28551	23313	1.18
2005	Gansu	3941847	25.92	3.17	101071	5160	124	58128	13450	30226	4198	229	31721	30839	34944	8727	1.17

2006	Guangdong	17952939	26.41	3.52	357650	15136	348	119634	161452	60743	27235	3722	124661	175520	63890	8715	1.37
2007	Guangxi	10219075	34.43	3.34	264485	12263	480	94666	111560	58971	11002	549	53729	175149	42500	5370	1.10
2008	Guizhou	6164328	28.39	3.12	159970	12522	41	65929	60006	34332	11785	440	44016	89287	28725	10464	1.15
2009	Hainan	1988812	23.78	3.42	45035	2592	51	26889	15458	4359	607	314	19912	12356	14449	910	1.22
2010	Hebei	17725642	30.74	3.40	454034	12232	203	338450	45232	73026	3484	6074	90952	165751	204531	5032	1.12
2011	Heilongjiang	7328148	22.67	2.63	230438	7764	526	152211	13711	54825	16851	604	26869	70838	130084	10411	1.17
2012	Henan	18087162	32.04	3.60	435993	14307	304	242151	151413	53669	2676	391	91696	240373	114219	4012	1.11
2013	Hubei	10290017	38.10	3.12	267951	11284	318	65151	136106	59020	18152	806	75159	150951	47125	6000	1.18
2014	Hunan	15931187	36.74	3.18	413160	16084	1397	107304	216464	90305	12926	2245	103618	225168	92116	8342	1.16
2015	Jiangsu	17597864	39.53	3.00	493818	16021	436	194665	224247	86379	2299	2249	99148	264939	142526	3226	1.15
2016	Jiangxi	12543925	33.57	3.54	283781	10796	1125	57795	138466	80093	17102	1121	144491	98662	45425	5999	1.20
2017	Jilin	4484285	22.51	2.70	139477	4710	1966	90313	10161	37025	6460	228	34567	30467	73754	5399	1.14
2018	Liaoning	5200437	26.23	2.75	168663	5618	94	100064	11565	51923	9229	1500	51280	52098	69815	1088	1.08
2019	Inner Mongolia	5919165	24.38	2.74	172725	9637	1622	124351	14566	41832	1422	191	43195	35332	90983	12852	1.17
2020	Ningxia	1041959	24.82	3.14	25273	1397	58	16542	2590	7308	176	54	6140	7109	12255	1166	1.24
2021	Qinghai	1237394	21.94	3.06	28364	1806	1694	15491	4641	9622	386	30	8482	9814	8928	2946	1.27
2022	Shaanxi	8394596	28.85	3.05	218969	10349	295	103810	63776	53427	6133	2172	61288	115983	30075	21972	1.20
2023	Shandong	19633371	32.14	3.03	555539	16773	117	412345	53861	102936	2235	935	105549	177664	274908	14191	1.13
2024	Shanghai	3391859	30.25	2.45	100049	3066	715	24233	44272	29262	638	4710	35992	46750	19423	950	1.33
2025	Shanxi	8098814	25.43	3.24	208837	7124	292	128133	41454	42626	2929	819	49930	87194	66418	12419	1.16
2026	Sichuan	16241360	34.47	2.80	494678	24545	2048	133695	170345	141458	64579	9146	144800	259633	80423	34367	1.11
2027	Tianjin	1605727	29.64	2.98	36626	688	6	20978	1965	12727	559	1085	5896	13066	18217	135	1.44
2028	Xinjiang	3536387	26.04	2.75	95090	2368	50	57285	7087	32598	301	187	31109	21827	34576	9946	1.32
2029	Tibet	444301	33.52	2.89	10835	1334	69	5712	5333	1058	39	27	5633	2406	2961	1169	1.26
2030	Yunnan	9949242	30.04	3.29	249892	15089	538	95990	113777	49076	5598	540	85728	73181	58444	47628	1.14
2031	Zhejiang	14035213	38.53	2.66	435571	17019	321	78393	215994	143891	9590	4722	88524	262572	92204	9290	1.16
	rural																
3001	Anhui	33860554	34.04	3.12	972114	12697	1032	594442	384935	5062	259	113	122416	440296	399437	22662	1.10
3002	Beijing	3289036	35.39	2.76	85494	2139	89	81788	2698	2877	93	177	2991	19546	63298	1798	1.36
3003	Chongqing	13078118	42.04	2.72	436237	8496	810	215548	219389	6337	3076	383	34275	160849	146892	102717	1.08
3004	Fujian	16018762	41.24	3.16	447940	13851	615	152099	279696	27946	1860	190	105558	152003	108638	95592	1.11
3005	Gansu	16451585	21.94	3.89	444734	2789	233	434394	12043	911	94	81	23583	50990	233241	139709	0.94
3006	Guangdong	38064798	25.99	3.74	825588	7932	862	473821	328499	27016	3542	642	168179	388958	244088	32295	1.22
3007	Guangxi	28011829	28.82	3.47	788492	7837	834	494076	294396	7474	300	83	100152	424443	210891	60843	1.01
3008	Guizhou	22784212	27.92	3.29	657275	13176	244	526145	137494	5485	1206	121	80232	208026	247780	134413	1.03
3009	Hainan	4359920	21.29	3.63	109378	771	69	101212	8248	437	217	35	22309	16584	68949	2307	1.09
3010	Hebei	41530827	30.09	3.50	1138877	6755	525	1108487	32754	3591	510	290	65563	351042	689663	39364	1.04
3011	Heilongjiang	17281672	20.92	3.19	472849	3926	1647	469755	3174	2668	1148	30	5933	44163	339849	86830	1.13
3012	Henan	58410084	32.23	3.58	1593259	18790	715	1263614	341472	6231	554	178	170146	778487	632719	30697	1.01
3013	Hubei	28154883	38.64	3.40	805308	11381	807	395220	405959	12191	2267	1052	87280	373421	286599	69389	1.01
3014	Hunan	37743917	34.27	3.54	1008324	9900	2170	496152	516168	5569	262	73	113888	408562	427367	68407	1.04
3015	Jiangsu	31993485	42.35	3.03	978352	13096	999	526012	444382	17344	893	2817	77218	494838	411206	8186	1.06
3016	Jiangxi	26200474	33.81	3.86	627420	6578	1410	251425	373710	8390	355	118	184327	209487	198186	41998	1.07
3017	Jilin	12896125	20.98	3.35	353543	2220	2523	347297	3170	4561	676	59	11283	35524	274007	34949	1.07
3018	Liaoning	16667944	25.95	3.12	519784	3994	237	512930	6643	3709	390	106	31856	123657	360371	7894	1.02
3019	Inner Mongolia	11371410	22.17	2.97	337168	4773	1167	331674	6301	3644	77	245	10616	34647	206674	90004	1.12

3020	Ningxia	3514019	22.12	3.54	86461	1371	35	80927	1965	4863	64	13	4944	9056	60381	13451	1.13
3021	Qinghai	3331549	18.51	4.06	71842	604	1521	69459	2789	181	7	10	2675	9718	36221	23832	1.11
3022	Shaanxi	20681076	31.22	3.54	572916	6711	497	481090	94599	3360	348	230	60338	235474	142395	141420	1.01
3023	Shandong	49111245	31.95	3.07	1549890	8748	182	1511164	40165	6807	399	103	77610	400711	1025247	55070	1.03
3024	Shanghai	2868506	38.83	2.37	90972	1752	1153	31644	57352	3415	49	264	8884	48551	33963	1326	1.29
3025	Shanxi	19383034	25.09	3.44	521669	4921	593	481296	38553	6348	290	103	34053	138101	243316	111120	1.07
3026	Sichuan	47509769	36.63	3.10	1625052	36122	3253	1067677	574735	16573	1425	764	147168	513785	611594	388627	0.92
3027	Tianjin	3005963	25.95	3.21	78318	570	30	74498	686	3345	110	249	2325	7772	68306	485	1.19
3028	Xinjiang	13519120	22.35	3.55	314397	2226	115	309505	2663	4345	82	28	11730	36704	207565	60624	1.20
3029	Tibet	2461371	27.55	4.95	44816	1260	718	27819	17858	360	26	13	2594	5152	23631	14699	1.06
3030	Yunnan	30970894	25.61	3.89	756974	10742	1276	461191	296513	6950	2470	592	68863	112129	239753	346971	1.04
3031	Zhejiang	22249067	49.12	2.67	740469	17587	807	152558	544733	58732	1649	384	60829	419761	236627	40839	1.10

Note: The three **urbanity attributes**, namely **urban/township/rural**, are represented by number 1/2/3 in the first column of this table; "**Prov_id**" refers to the ID number of each province; "**Aver. pop. per family**" refers to the average number of population per family; "**Amp. factor**" refers to the amplification factor used to amplify the building related statistics from 2010 to 2015 (see **Sect. 2.1** and **2.4.1** for more details).

930

Table 3: The population proportions and thresholds used for each province to assign the grids in the 2015 GHSL profile with urban/township/rural attributes.

Province	Province ID	2010-census recorded population in each urbanity				Population proportion			Population threshold (PT)	
		urban	township	rural	sum	urban	township	rural	PT1 (urban/township)	PT2 (township/rural)
Anhui	01	12182587	13394530	33923351	59500468	20.47%	22.51%	57.01%	13950	6907
Beijing	02	15563215	1295477	2753676	19612368	79.35%	6.61%	14.04%	2702	1775
Chongqing	03	8681611	6614192	13550367	28846170	30.10%	22.93%	46.97%	11194	5412
Fujian	04	12548384	8513556	15832277	36894217	34.01%	23.08%	42.91%	6020	2586
Gansu	05	5258935	3932250	16384078	25575263	20.56%	15.38%	64.06%	15167	9337
Guangdong	06	52388382	16641873	35290204	104320459	50.22%	15.95%	33.83%	5229	2996
Guangxi	07	8352777	10065066	27605918	46023761	18.15%	21.87%	59.98%	11694	5065
Guizhou	08	5537562	6199971	23011023	34748556	15.94%	17.84%	66.22%	18152	10413
Hainan	09	2324288	1984228	4362969	8671485	26.80%	22.88%	50.31%	8256	3679
Hebei	10	14388021	17187307	40278882	71854210	20.02%	23.92%	56.06%	5682	2403
Heilongjiang	11	14122516	7201199	16990276	38313991	36.86%	18.80%	44.34%	3848	1485
Henan	12	18331493	17888274	57810172	94029939	19.50%	19.02%	61.48%	15199	8456
Hubei	13	17928160	10516925	28792642	57237727	31.32%	18.37%	50.30%	11667	6345
Hunan	14	12738442	15714621	37247699	65700762	19.39%	23.92%	56.69%	13552	5876
Jiangsu	15	30166466	17205022	31289453	78660941	38.35%	21.87%	39.78%	6559	3341
Jiangxi	16	7504291	11995669	25067837	44567797	16.84%	26.92%	56.25%	11326	3400
Jilin	17	10196745	4451454	12804616	27452815	37.14%	16.21%	46.64%	6168	2866
Liaoning	18	22021184	5166779	16558360	43746323	50.34%	11.81%	37.85%	3511	1882
Inner Mongolia	19	8011564	5708610	10986117	24706291	32.43%	23.11%	44.47%	11152	5036
Ningxia	20	2059295	962727	3279328	6301350	32.68%	15.28%	52.04%	11659	7624
Qinghai	21	1368033	1148221	3110469	5626723	24.31%	20.41%	55.28%	11850	5113
Shaanxi	22	8837175	8222162	20268042	37327379	23.67%	22.03%	54.30%	13731	6872
Shandong	23	28364984	19255743	48171992	95792719	29.61%	20.10%	50.29%	6577	3372
Shanghai	24	17640842	2914256	2464098	23019196	76.64%	12.66%	10.70%	4936	2750
Shanxi	25	9414053	7746486	18551562	35712101	26.36%	21.69%	51.95%	8804	3890
Sichuan	26	15915660	16428768	48073100	80417528	19.79%	20.43%	59.78%	14668	8123
Tianjin	27	8858126	1419767	2660800	12938693	68.46%	10.97%	20.56%	3138	1872
Xinjiang	28	6071803	3263949	12480063	21815815	27.83%	14.96%	57.21%	10473	3620
Tibet	29	272322	408267	2321576	3002165	9.07%	13.60%	77.33%	9751	4522
Yunnan	30	6324830	9634242	30007694	45966766	13.76%	20.96%	65.28%	19028	8699
Zhejiang	31	20386294	13163915	20876682	54426891	37.46%	24.19%	38.36%	5599	2513

Note: For each province, "**PT1(urban/township)**" and "**PT2 (township/rural)**" are the population thresholds to assign the grids in the 2015 GHSL profile with urban/township/rural attributes. According to the population density λ in each grid, the assignment criteria are that: if $\lambda \geq PT1$, the grid is assigned as **urban**; if $PT1 > \lambda \geq PT2$, **township**; *if $\lambda < PT2$, **rural** (see context in **Sect. 2.3** for more details).

Table 4: Average unit construction price (per m^2) for each of the 17 building subtypes used in this paper.

Structure type	Storey class	Building subtype abbreviation	Unit construction price (RMB/m^2 in 2015 current price)
brick/wood	1	BRIWOMC1	2050
	2-3	BRIWOMC23	2350
steel/RC	1	STLRCMC1	3700
	2-3	STLRCMC23	3900
	4-6	STLRCMC46	4100
	7-9	STLRCMC79	4300
	≥10	STLRCMC10	4500
mixed	1	MIXEDMC1	2800
	2-3	MIXEDMC23	3000
	4-6	MIXEDMC46	3200
	7-9	MIXEDMC79	3400
	≥10	MIXEDMC10	3600
other	1	OTHERMC1	2600
	2-3	OTHERMC23	2800
	4-6	OTHERMC46	3000
	7-9	OTHERMC79	3200
	≥10	OTHERMC10	3400

935

Table 5: The modeled floor area and replacement value of residential buildings in urban/township/rural urbanity of the 31 provinces in mainland China.

Province ID	Province name	Modeled residential building floor area (**million m²**) in each urbanity level			Modeled residential building replacement value (**billion RMB**, in 2015 current price) in each urbanity level		
		urban	township	rural	urban	township	rural
01	Anhui	357	431	1150	507	498	1080
02	Beijing	516	51	117	1920	147	223
03	Chongqing	250	222	550	564	428	825
04	Fujian	377	326	667	1000	648	1240
05	Gansu	141	102	351	231	114	259
06	Guangdong	1640	448	864	4130	798	1060
07	Guangxi	260	350	808	618	691	1160
08	Guizhou	143	175	635	221	197	487
09	Hainan	60	47	86	141	79	89
10	Hebei	448	544	1210	916	880	1370
11	Heilongjiang	341	166	360	844	257	365
12	Henan	630	580	1880	1120	1020	2550
13	Hubei	582	392	1090	1270	610	1400
14	Hunan	431	583	1290	749	786	1360
15	Jiangsu	1040	695	1350	3250	1910	3130
16	Jiangxi	234	419	884	387	533	845
17	Jilin	258	100	266	1080	268	483
18	Liaoning	572	136	426	2080	353	710
19	Inner Mongolia	206	143	247	1170	485	559
20	Ningxia	63	26	78	185	56	121
21	Qinghai	41	26	60	107	55	87
22	Shaanxi	260	242	644	597	523	960
23	Shandong	936	632	1530	2450	1380	2480
24	Shanghai	516	102	109	2120	339	254
25	Shanxi	255	206	484	661	361	587
26	Sichuan	483	556	1740	795	780	1780
27	Tianjin	255	48	78	1000	204	217
28	Xinjiang	184	92	299	516	206	279
29	Tibet	9	15	67	25	35	83
30	Yunnan	221	312	767	334	431	727
31	Zhejiang	673	542	1090	1820	1200	1910
In total:		12400	8710	21200	32808	16300	28700

Note: (a) In this paper, for each of the 17 building subtypes in each grid, the same unit construction price is used to derive the replacement value in different urbanities and provinces; (b) The modeled floor area and replacement value are for residential buildings (see context in **Sect. 3.1.1** for more details).

940

Table 6: The regression parameters and correlation coefficients for population and floor area in each province.

Province ID	Province name	Pop_a	Pop_b	Pop_R^2	FloorArea_a	FloorArea_b	Area_R^2
01	Anhui	1.227	-121096	0.9525	1.2256	-4000000	0.917
02	Beijing	1.4375	-11276	0.9986	1.4947	-3000000	0.9993
03	Chongqing	1.1261	-68344	0.9624	1.2336	-6000000	0.9049
04	Fujian	1.2485	-66004	0.9741	0.9975	2000000	0.8165
05	Gansu	1.1977	-38495	0.9876	1.1499	-651568	0.9526
06	Guangdong	1.5014	-212584	0.9712	1.6419	-9000000	0.9285
07	Guangxi	0.936	43874	0.9251	0.9482	993643	0.8633
08	Guizhou	1.1151	-37198	0.99	1.2213	-2000000	0.961
09	Hainan	1.2608	-80398	0.9692	1.2068	-2000000	0.9675
10	Hebei	1.1402	-27316	0.9832	1.05	184103	0.9276
11	Heilongjiang	1.1307	-30556	0.9839	1.0486	118704	0.977
12	Henan	1.1817	-93834	0.9599	1.0788	-554637	0.9039
13	Hubei	1.2252	-101914	0.9788	1.374	-7000000	0.9387
14	Hunan	1.1237	-212458	0.9628	1.032	6000000	0.8858
15	Jiangsu	1.3726	-266170	0.9335	1.2612	6000000	0.7783
16	Jiangxi	1.1411	-18384	0.9901	1.0855	252638	0.9365
17	Jilin	1.0739	-16159	0.9907	0.9804	715875	0.9894
18	Liaoning	1.1467	-273787	0.9957	1.0608	-933912	0.9902
19	Inner Mongolia	1.1574	-11718	0.9814	1.1262	-162051	0.978
20	Ningxia Hui	1.2559	-37867	0.9668	1.0727	507343	0.9588
21	Qinghai	1.1457	-1152.1	0.9935	0.9763	377230	0.9851
22	Shaanxi	1.2448	-53315	0.9857	1.2304	-1000000	0.9459
23	Shandong	1.1272	-35525	0.9725	1.0518	392271	0.934
24	Shanghai	1.1752	286962	0.9665	1.2034	6000000	0.9368
25	Shanxi	1.2375	-38478	0.9904	1.1738	-474998	0.9456
26	Sichuan	1.175	-478703	0.9754	1.0902	-7000000	0.9561
27	Tianjin	1.1832	274914	0.8724	1.2782	4000000	0.8993
28	Xinjiang	1.1519	-2241.9	0.9827	1.1454	-10818	0.9789
29	Tibet	1.2168	-3498.3	0.9834	1.1196	-1699.8	0.9199
30	Yunnan	1.1632	-26658	0.9898	0.9589	1000000	0.9083
31	Zhejiang	1.2686	-45842	0.9751	1.323	-4000000	0.88

Note: "**Pop_a**" and "**Pop_b**" are the linear regression parameters between the 2015 GHSL population and the 2010-census recorded population; "**FloorArea_a**" and "**FloorArea_b**" are the linear regression parameters between the modeled residential building floor area in this paper and that extracted from the 2010-census records; "**Pop_R^2**" and "**FloorArea_R^2**" are the correlation coefficients of population and floor area, respectively. For Hunan, Liaoning, and Sichuan provinces, the population and floor area comparisons are compared at the prefecture-level; while for the other 28 provinces, the population and floor area comparisons are at the county-level. The correlation analysis figures for each of the 31 provinces are available from the online supplement (see the context in **Sect. 3.2.2** for more details).

945

Appendix A

950   For each grid, to derive the population living in each of the 17 building subtypes (their abbreviations are given in Table 4), namely the 17 to-be-solved variables on the left side of the equation set in Sect. 2.4.2., a series of distribution steps based on a prioritized ranking of building types and storey classes are used in this paper. A MATLAB script and an input file illustrating the distribution processes are also available from the online supplement. With the help of the MATLAB script, it will be easier to understand the distribution steps as follows.

955   (1)   For brick/wood structure type, in each grid if $Num_{BRIWO} < Num_{storey1}$, the population living in brick/wood structure types (Num_{BRIWO}) is first placed into the 1-storey class, then we get $BRIWOMC1 = Num_{BRIWO}$ and the remaining population living in brick/wood structure type is 0, while the remaining population living in the 1-storey class is ($Num_{storey1} - Num_{BRIWO}$); but if $Num_{BRIWO} \geq Num_{storey1}$, then the population living in the 1 storey class buildings ($Num_{storey1}$) are assumed to be in brick/wood structure type, we get

960        $BRIWOMC1 = Num_{storey1}$ and the remaining population living in brick/wood buildings is ($Num_{BRIWO} - Num_{storey1}$), while the remaining population living in the 1-storey class is 0;

   (2)   If the remaining population living in brick/wood buildings ($Num_{BRIWO} - Num_{storey1}$) $< Num_{storey23}$, then they are placed into 2-3 storey class and we get $BRIWOMC23 = Num_{BRIWO} - BRIWOMC1$ or $BRIWOMC23 = Num_{BRIWO} - Num_{storey1}$, and the remaining population in the 2-3 storey class is

965   ($Num_{storey23} - (Num_{BRIWO} - Num_{storey1})$); but if ($Num_{BRIWO} - Num_{storey1}$) $\geq Num_{storey23}$, we directly assign $BRIWOMC23 = Num_{storey23}$ and the remaining population living in brick/wood buildings is ($Num_{BRIWO} - Num_{storey1} - Num_{storey23}$);

   (3)   For steel/RC structure type, in each grid if $Num_{STLRC} < Num_{storey \geq 10}$, the population living in steel/RC structure type (Num_{STLRC}) is first placed in the ≥ 10 storey class, and we get $STLRCMC10 = Num_{STLRC}$,

970   then the remaining population living in the ≥ 10 storey class is ($Num_{storey \geq 10} - Num_{STLRC}$), while the remaining population living in steel/RC structure type is 0; but if $Num_{STLRC} \geq Num_{storey \geq 10}$, then we directly assign $STLRCMC10 = Num_{storey \geq 10}$, and the remaining population living in steel/RC structure type is ($Num_{STLRC} - Num_{storey \geq 10}$), while the remaining population living in ≥ 10 storey class is 0;

   (4)   Following the above step (3), if $Num_{STLRC} \geq Num_{storey \geq 10}$, the remaining population living in steel/RC

975   structure type is compared with the population living in other storey class and distributed into the remaining storey classes from the highest to the lowest, assuming that the least population in steel/RC would be in the 1-storey class, then we get $STLRCMC79 = Num_{STLRC} - Num_{storey \geq 10}$ or $STLRCMC79 = Num_{storey79}$ or $STLRCMC79 = 0$; $STLRCMC46 = Num_{STLRC} - Num_{storey \geq 10} - Num_{storey79}$ or $STLRCMC46 = Num_{storey46}$ or $STLRCMC46 = 0$; $STLRCMC23 = Num_{STLRC} - Num_{storey \geq 10} - Num_{storey79} -$

980        $Num_{storey46}$ or $STLRCMC23 = Num_{storey23} - (Num_{BRIWO} - Num_{storey1})$ or $STLRCMC23 = 0$; $STLRCMC1 = Num_{STLRC} - Num_{storey \geq 10} - Num_{storey79} - Num_{storey46} - (Num_{storey23} - (Num_{BRIWO} - Num_{storey1}))$ or $STLRCMC1 = (Num_{storey1} - Num_{BRIWO})$ or $STLRCMC1 = 0$;

(5) After getting the population living in 7 building subtypes ($BRIWOMC1$, $BRIWOMC23$, $STLRCMC10$, $STLRCMC79$, $STLRCMC46$, $STLRCMC23$, $STLRCMC1$) and the remaining population living in each of the five storey classes determined, to derive the population living in storey class with structure type "mixed" and "other", we assume that the populations living in the five storey classes of "mixed" structure type are equal to the product of the remaining population in each storey class and the ratio of $Num_{MIXED}/(Num_{MIXED} + Num_{OTHER})$; similarly, the populations living in the five storey classes of "other" structure type are equal to the product of the remaining population in each storey class and the ratio of $Num_{OTHER}/(Num_{MIXED} + Num_{OTHER})$.